PERGAMON

Chemical Engineering Science 57 (2002) 5083–5114

Chemical Engineering Science

www.elsevier.com/locate/ces

Dynamic optimization of dissipative PDE systems using nonlinear order reduction

Antonios Armaou[1], Panagiotis D. Christofides*

Department of Chemical Engineering, University of California, LA, 5531 Boelter Hall, 405 Hilgard Avenue, Los Angeles, CA 90095-1592, USA

Received 11 October 2001; received in revised form 12 June 2002; accepted 15 July 2002

Abstract

This article presents computationally efficient methods for the solution of *dynamic* constraint optimization problems arising in the context of spatially distributed processes governed by highly dissipative nonlinear partial differential equations (PDEs). The methods are based on spatial discretization using the method of weighted residuals with spatially global basis functions (i.e., functions that cover the entire domain of definition of the process and satisfy the boundary conditions). More specifically, we perform spatial discretization of the optimization problems using the method of weighted residuals with analytical or empirical (obtained via Karhunen–Loève expansion) eigenfunctions as basis functions, and combination of the method of weighted residuals with approximate inertial manifolds. The proposed methods account for the fact that the dominant dynamics of highly dissipative PDE systems are low dimensional in nature and lead to approximate optimization problems that are of significantly lower order compared to the ones obtained from spatial discretization using finite-difference and finite-element techniques, and thus, they can be solved with significantly smaller computational demand. The resulting dynamic nonlinear programs include equality constraints that constitute a low-order system of coupled ordinary differential equations and algebraic equations, which can then be solved with combination of standard temporal discretization and nonlinear programming techniques. We employ backward finite differences (implicit Euler) to perform temporal discretization and solve the nonlinear programs resulting from temporal and spatial discretization using reduced gradient techniques (MINOS). We use two representative examples of dissipative PDEs, a diffusion-reaction process with constant and spatially varying coefficients, and the Kuramoto–Sivashinsky equation, a model that describes incipient instabilities in a variety of physical and chemical systems, to demonstrate the implementation and evaluate the effectiveness of the proposed optimization algorithms.

Keywords: Highly dissipative partial differential equations; Method of weighted residuals; Karhunen–Loève expansion; Approximate inertial manifolds; Reduced gradient optimization methods; Spatially distributed processes

1. Introduction

Many important processes in chemical engineering involve coupling of complex chemical reactions with significant mass and energy transport mechanisms. Examples include plasma-enhanced chemical vapor deposition and etching, as well as, metal organic vapor phase epitaxy (MOVPE), which are used in semiconductor manufacturing. Models for transport-reaction processes can be derived from dynamic conservation equations and are described by highly dissipative (typically parabolic) partial differential equation (PDE) systems. The design of such processes is usually addressed assuming steady-state operating conditions. However, there are instances where more efficient process operation can be accomplished through time-varying operation. Examples include the horizontal MOVPE process where the reactants' concentration at the inflow to the reactor is varied with time to grow the desired heterostructures on the wafer. In the case of the MOVPE, the optimal process design problem may be formulated as a dynamic nonlinear program whose objective is to find the optimal concentration time profiles of the reactants at the inflow that maximize the deposition rate on the wafer subject to equality constraints that include mass, energy and momentum conservation equations, and inequality

* Corresponding author.
E-mail address: pdc@seas.ucla.edu (P. D. Christofides).
[1] Present address: Department of Chemical Engineering, The Pennsylvania State University, University Park, PA 16802-4400, USA.

0009-2509/02/$ - see front matter © 2002 Elsevier Science Ltd. All rights reserved.
PII: S0009-2509(02)00419-0

constraints for the microstructure and spatial uniformity of the deposited structure.

The standard approach for the solution of dynamic nonlinear programs (NLPs) with PDE constraints involves the discretization of the spatial and temporal domain using finite-element or finite-difference techniques and subsequently the solution of the resulting large-scale nonlinear program using optimization techniques for sparse NLPs, such as reduced gradient and reduced successive quadratic programming methods (see, for example, Vasantharajan, Viswanathan, & Biegler, 1990; Manousiouthakis & Sourlas, 1992; Floudas & Panos, 1992; Biegler, Nocedal, & Schmid, 1995). This approach has been successfully used to solve several optimization problems arising in the context of various distributed parameter system applications (see, for example, Borggaard & Burns, 1997; Turgeon, Pelletier, & Borggaard, 2000). One potential drawback of this approach is that the nonlinear program resulting from the temporal and spatial discretization may be of very high-order (in order to compute the optimal solution with the desired accuracy), and thus, it may not be very efficient computationally. The main reason for this is that a brute force discretization with finite differences/elements does not account for the inherent characteristics of the PDE equality constraints.

Highly dissipative PDE systems, arising in the context of transport-reaction processes and of several fluid dynamic systems, are characterized by dominant dynamics which are low-dimensional in nature and can be captured by low-dimensional ordinary differential equation models. One approach to solve optimization problems with dissipative PDE equality constraints, while accounting for the inherent characteristics of the PDEs in the discretization process, is to use Galerkin's method with the eigenfunctions of the linear spatial differential operator as basis functions for the discretization. This approach is motivated from the fact that the main feature of highly dissipative PDEs is that the dominant structure of their solutions is usually characterized by a finite (typically small) number of degrees of freedom (Temam, 1988) (for example, in the case of parabolic PDE systems with linear spatial differential operators, this follows from the fact that the eigenspectrum of the spatial differential operator can be partitioned into a finite-dimensional slow one and an infinite-dimensional stable fast complement, Christofides, 2001). Even though, this approach may significantly reduce the dimension of the optimization problem which results from the spatial discretization for few specific types of differential operators for which the eigenfunction expansions converge quickly (note that for general Sturm–Liouville operators such eigenfunction expansions converge very slowly), it may not be very efficient for problems that involve nonlinear spatial differential operators (e.g., nonlinear dependence of the diffusion coefficient and thermal conductivity on temperature) and spatially varying coefficients. The reason is that the eigenvalue problems of nonlinear spatial differential operators cannot be, in general, solved analytically, and thus it is difficult to a priori (without having any information about the solution of the system) choose an optimal (in the sense that will lead to an accurate and low-order approximation) basis to expand the solution of the PDE system. An approximate way to address this problem (Ray, 1981) is to linearize the nonlinear spatial differential operator around a steady state and address the optimization problem on the basis of the resulting quasi-linear system. However, this approach is only valid in a small neighborhood of the steady state where the linearization takes place.

To overcome this limitation, we recently employed (Bendersky & Christofides, 1999, 2000) an alternative approach to the solution of steady-state optimization programs arising in the context of transport-reaction processes (described by parabolic PDEs) which is based on spatial discretization using the method of weighted residuals with empirical eigenfunctions as basis functions. The empirical eigenfunctions are constructed by applying Karhunen–Loève (K–L) expansion (Lumley, 1981; Sirovich, 1987a, b) (also known as proper orthogonal decomposition, method of empirical eigenfunctions and principal component analysis) to process solution data. This approach to spatial discretization takes into consideration the presence of dominant spatial patterns in the solution of the parabolic PDEs and leads to reduced-order NLPs that can be solved significantly faster compared to NLPs resulting from spatial discretization using the finite-difference method (see Bendersky & Christofides, 2000, for detailed comparisons). Order reduction of PDE systems, based on data-based construction of the basis functions, has been extensively used in recent years in the context of feedback control of parabolic PDE systems (Shvartsman & Kevrekidis, 1998; Mahadevan & Hoo, 2000; Baker & Christofides, 2000). In King and Sachs (2000), an approach, based on semi-definite programming, is used to construct reduced-order approximations of controllers for parabolic PDEs. The reader may also refer to (Marquardt, 2002) for an excellent review of results in the broad area of order reduction of large-scale dynamic systems.

In this work, we present computationally efficient methods for the solution of *dynamic* constraint optimization problems arising in the context of spatially distributed processes governed by highly dissipative nonlinear PDEs. The methods are based on spatial discretization using the method of weighted residuals with spatially global basis functions (i.e., functions that cover the entire domain of definition of the process and satisfy the boundary conditions). More specifically, we perform spatial discretization of the optimization problems using the method of weighted residuals with analytical or empirical (obtained via Karhunen–Loève expansion) eigenfunctions as basis functions, and combination of the method of weighted residuals with approximate inertial manifolds. In the case of performing order reduction through spatial discretization using empirical eigenfunctions as basis functions, we initially form an ensemble of "snapshots" of the

solutions of the PDE system for different initial conditions and input profiles. We then apply Karhunen–Loève expansion to this ensemble to derive the set of empirical eigenfunctions, which are subsequently used for order reduction. In the case of performing order reduction through combination of the method of weighted residuals with approximate inertial manifolds, we take advantage of the fact that the dynamics of the higher-order modes in highly dissipative PDEs decay very fast to obtain low-order approximate nonlinear programs. Both spatial discretization approaches account for the fact that the dominant dynamics of highly dissipative PDE systems are low dimensional in nature and lead to approximate dynamic nonlinear programs whose equality constraints constitute a low-order system of coupled ordinary differential equations and algebraic equations (DAEs) which can then be solved with combination of standard temporal discretization and nonlinear programming techniques. We use backward finite-differences to perform temporal discretization (implicit Euler) and solve the finite-dimensional nonlinear programs resulting from temporal and spatial discretization using MINOS.

Two representative examples of dissipative PDEs, a diffusion-reaction process with nonlinearities and spatially varying coefficients, and the Kuramoto–Sivashinsky equation, a model that describes incipient instabilities in a variety of physical and chemical systems, are used to demonstrate the implementation and evaluate the effectiveness of the proposed optimization algorithms. The proposed methods are used to determine the inputs needed to optimize meaningful performance indices that involve penalty on the PDE process response and inputs, in the presence of constraints in the magnitude of the inputs.

2. Formulation of the optimization problem

We focus on spatially distributed processes modeled by highly dissipative PDE systems with the following state–space description:

$$\frac{\partial x}{\partial t} = \mathscr{A}(x) + f(t,x,d) \tag{1}$$

subject to the mixed-type boundary conditions:

$$q\left(x, \frac{\mathrm{d}x}{\mathrm{d}\eta}, \ldots, \frac{\mathrm{d}^{n_o-1}x}{\mathrm{d}\eta^{n_o-1}}\right) = 0 \quad \text{on } \Gamma \tag{2}$$

and the initial condition

$$x(z,0) = x_0(z). \tag{3}$$

In the above PDE system, $x(z,t) \in \mathbb{R}^n$ denotes the vector of state variables, $t \in [0, t_f]$ is the time (t_f is the terminal time), $z = [z_1, z_2, z_3] \in \Omega \subset \mathbb{R}^3$ is the vector of spatial coordinates, Ω is the domain of definition of the process and Γ its boundary. $\mathscr{A}(x)$ is a dissipative, possibly nonlinear, spatial differential operator which includes higher-order spatial derivatives, $f(t,x,d)$ is a nonlinear, possibly time varying, vector function which is assumed to be sufficiently smooth with respect to its arguments, $d(t) \in \mathbb{R}^p$ is the vector of design variables which are assumed to be piecewise continuous functions of time, $q(x, \mathrm{d}x/\mathrm{d}\eta, \ldots, \mathrm{d}^{n_o-1}x/\mathrm{d}\eta^{n_o-1})$ is a nonlinear vector function which is assumed to be sufficiently smooth (n_o is the order of the PDE of Eq. (1)), $\mathrm{d}x/\mathrm{d}\eta|_\Gamma$ denotes the derivative in the direction perpendicular to the boundary and $x_0(z)$ is a smooth vector function of z. Since we are dealing with dissipative PDE systems that model spatially distributed processes, we assume that for a given set of initial and boundary conditions and for each piecewise continuous vector function, $d(t) \in \mathbb{R}^p$, the system of Eq. (1) has a unique solution. The mathematically delicate questions of existence and uniqueness of solutions for Eq. (1) are beyond the scope of this work. Throughout the paper, we will make use of the inner product and norm in $L_2[\Omega]$ (where $L_2[\Omega]$ is the space of square integrable functions which are defined in Ω), which are defined, respectively, as

$$(\phi_1, \phi_2) = \int_\Omega \phi_1(z)\phi_2(z)\,\mathrm{d}z, \qquad \|\phi_1\|_2 = (\phi_1, \phi_1)^{1/2}, \tag{4}$$

where ϕ_1, ϕ_2 are two elements of $L_2[\Omega]$.

Systems of the form of Eq. (1) can model the vast majority of dynamic spatially distributed processes including both transport-reaction processes and several classes of dissipative fluid dynamic systems (see application examples in Sections 3 and 5 below). The nonlinear structure of the spatial differential operator, $\mathscr{A}(x)$, allows accounting for explicit dependence of diffusivities and thermal conductivities on temperature and concentration in certain transport-reaction processes, while the nonlinear term $f(t,x,d)$ allows modeling complex reaction mechanisms. Furthermore, the assumption that the design variables enter the system through the term $f(t,x,d)$ is usually satisfied; for example, when $d(t)$ models inputs used to influence the dynamic behavior of the PDE system (see the examples in Sections 3 and 5 below).

A general optimization problem for the system of Eqs. (1)–(3) can be formulated as follows:

$$\begin{aligned}
\min \quad & \int_0^{t_f} \int_\Omega G(x(z,t), d(t))\,\mathrm{d}z\,\mathrm{d}t \\
\text{s.t.} \quad & -\frac{\partial x}{\partial t} + \mathscr{A}(x) + f(t,x,d) = 0, \\
& x(z,0) = x_0(z), \\
& q\left(x, \frac{\mathrm{d}x}{\mathrm{d}\eta}, \ldots, \frac{\mathrm{d}^{n_o-1}x}{\mathrm{d}\eta^{n_o-1}}\right) = 0 \quad \text{on } \Gamma, \\
& g(x,d) \leqslant 0, \quad \forall z \in \Omega, \ t \in [0, t_f],
\end{aligned} \tag{5}$$

where $\int_0^{t_f}\int_\Omega G(x,d)\,dz\,dt$ is the objective function and $g(x,d)$ is the vector of inequality constraints which may include bounds on the state and design variables. Both $G(x,d)$ and $g(x,d)$ are assumed to be sufficiently smooth functions of their arguments. Since the focus of this work is on the development of computationally efficient algorithms for solving dynamic nonlinear programs of the form of Eq. (5) through advanced spatial discretization techniques, we will make no assumption of convexity of the problem functions and of the feasible region, and therefore, we will focus throughout the manuscript on the computation of a local optimum. Global optimization techniques (e.g., (Floudas & Panos, 1992; Manousiouthakis & Sourlas, 1992)) can be applied on the finite-dimensional programs that result from the spatio-temporal discretization of the nonlinear program of Eq. (5) but such a study is beyond the scope of the present work. We note that the proposed approaches for computing a locally optimal solution of the program of Eq. (5) can be also applied to nonlinear programs, that include coupled nonlinear dissipative PDEs and nonlinear algebraic equality constraints, as well as explicit dependence of the functions G, f, g on the temporal and spatial coordinates, t, z. Finally, we note that the assumptions that we impose on the functions involved in the cost and the constraints are not sufficient to ensure the existence of a smooth $d(t)$; the study of this question is outside of the scope of the present manuscript.

Owing to the presence of the nonlinear PDE equality constraint of Eq. (1), the optimization problem of Eq. (5) cannot be solved directly. As a result, spatial and temporal discretization schemes should be employed to reduce the PDE system of Eq. (1) into a set of algebraic equations. The standard approach to address this problem is to utilize finite differences or finite elements to perform the spatial discretization, then discretize the temporal domain using collocation or finite difference techniques, and finally solve the resulting finite-dimensional nonlinear program using optimization techniques for sparse NLPs. The main disadvantage of this approach is that the number of nonlinear algebraic constraints resulting from these discretizations, which yields an acceptable approximation, may be very large, thereby leading to a computationally expensive optimization problem.

Motivated by this, we develop computationally efficient methods for the solution of the optimization problem of Eq. (5). We will begin with the development of an optimization method for solving the nonlinear program of Eq. (5) using an off-the-shelf set of global basis functions. We will continue with the data-based construction and use of empirical eigenfunctions as basis functions, and the combination of global basis functions with the concept of approximate inertial manifolds. We will use several examples of dissipative PDEs to demonstrate the implementation and evaluate the effectiveness of the proposed optimization algorithms.

3. Solution of optimization problem through spatial discretization with global basis functions

3.1. Computation of approximate nonlinear programs

In this subsection, we derive low-order approximations of the infinite-dimensional nonlinear program of Eq. (5) by using the method of weighted residuals. The central idea of the method of weighted residuals (see, Finlayson, 1980 for a comprehensive review of this method) is to approximate the exact solution of $x(z,t)$ by an infinite series of orthogonal basis functions (that form a complete set) defined on Ω with time-varying coefficients, substitute the series expansion into Eq. (1) to form the residual, and then force the residual to be orthogonal to a complete set of weighting functions (i.e., the inner product of the residual with a complete set of weighting functions in $L_2[\Omega]$ is set equal to zero) to compute a set of equations whose unknowns are the coefficients of the series expansion of the solution.

We present an application of this method to the optimization program of Eq. (5) for the case of $n=1$ (to simplify the notation). We initially expand the solution $x(z,t)$ in an infinite series in terms of a complete set of basis functions $\phi_k(z)$ as follows:

$$x(z,t)=\sum_{k=1}^{\infty} a_k(t)\phi_k(z), \tag{6}$$

where $a_k(t)$ are time-varying coefficients. Substituting the expansion of Eq. (6) into Eq. (5), multiplying the PDE and the inequality constraints with the weighting functions, $\psi_v(z)$, and integrating over the entire spatial domain (i.e., taking inner product in $L_2[\Omega]$ with the weighting functions), the following infinite-dimensional dynamic nonlinear program is obtained

$$\begin{aligned}
\min\quad & \int_0^{t_f}\int_\Omega G\left(\sum_{k=1}^{\infty} a_k(t)\phi_k(z), d\right) dz\,dt\\
\text{s.t.}\quad & -\sum_{k=1}^{\infty}\dot{a}_k\left(\int_\Omega \psi_v(z)\phi_k(z)\,dz\right)\\
&\quad +\int_\Omega \psi_v(z)\mathscr{A}\left(\sum_{k=1}^{\infty} a_k(t)\phi_k(z)\right)dz\\
&\quad +\int_\Omega \psi_v(z) f\left(t,\sum_{k=1}^{\infty} a_k(t)\phi_k(z), d\right)dz=0,\\
& V=1,\ldots,\infty,\\
& \int_\Omega \psi_v(z) g\left(\sum_{k=1}^{\infty} a_k(t)\phi_k(z), d\right)dz\leqslant 0,\\
& V=1,\ldots,\infty.
\end{aligned} \tag{7}$$

Truncating the series expansion of $x(z,t)$ up to order N and keeping the first N equations (i.e. $v=1,\ldots,N$), the infinite-dimensional program of Eq. (7) reduces to the following one with ODE equality constraints, where

the optimization parameters are the design variables $d(t)$ and the time varying coefficients $a_{kN}(t)$:

$$\begin{aligned}
\min \quad & \int_0^{t_f} \int_\Omega G\left(\sum_{k=1}^{N} a_{kN}(t)\phi_k(z), d\right) \mathrm{d}z\,\mathrm{d}t \\
\text{s.t.} \quad & -\sum_{k=1}^{N} \dot{a}_{kN}\left(\int_\Omega \psi_v(z)\phi_k(z)\,\mathrm{d}z\right) \\
& + \int_\Omega \psi_v(z)\mathscr{A}\left(\sum_{k=1}^{N} a_{kN}(t)\phi_k(z)\right)\mathrm{d}z \\
& + \int_\Omega \psi_v(z) f\left(t, \sum_{k=1}^{N} a_{kN}(t)\phi_k(z), d\right)\mathrm{d}z = 0, \\
& V = 1,\ldots,N, \\
& \int_\Omega \psi_v(z) g\left(\sum_{k=1}^{N} a_{kN}\phi_k(z), d\right)\mathrm{d}z \leqslant 0, \\
& V = 1,\ldots,N.
\end{aligned} \tag{8}$$

where $a_{kN}(t)$ is the approximation of $a_k(t)$ obtained by an Nth-order truncation. From Eq. (8), it is clear that the form of the algebraic equality and inequality depends on the choice of the weighting functions, as well as on N. The weighting functions determine the type of weighted residual method being used (see Remark 1).

Owing to the smoothness of the functions $G(x,d)$, $\mathscr{A}(x)$, $f(t,x,d)$, $g(x,d)$ and the completeness of the set of basis functions, $\phi_k(z)$, the nonlinear program of Eq. (8) is a well-defined approximation of the infinite-dimensional program Eq. (5); this is important for computing an accurate solution of the nonlinear program of Eq. (8) based on a low-dimensional nonlinear program (see algorithm in the next section) and is verified through numerical simulations in the three application studies considered in this work. The detailed mathematical study of the issue of convergence of the solution of the approximate nonlinear program of Eq. (8) to the one of the infinite-dimensional program of Eq. (5) as $N \to \infty$ requires constraining the type of nonlinearities considered and is outside of the scope of this work; the reader may refer, for example, to Temam (1988), Miletta (1994) and Christofides (2001) for various results on approximation of infinite-dimensional systems with finite-dimensional systems.

Remark 1. When the number of basis functions, $\phi_k(z)$, required to obtain a good approximation (measured in a desired norm) of the solution of the system of partial differential equations (equality constraints), is small, the weighting functions are usually chosen to be identical to the basis functions, in which case the method of weighted residuals reduces to Galerkin's method.

Remark 2. Referring to the order reduction of the PDE system, it is important to note that it accounts for both the diffusion and convection phenomena (modeled by the nonlinear spatial differential operator) and the reaction phenomena (modeled by the nonlinear term $f(t,x,d)$). Therefore, the resulting finite-dimensional model not only approximates the diffusion and convection phenomena but it also approximates the reaction phenomena.

Remark 3. We note that an alternative approach to perform spatial discretization of the infinite dimensional program of Eq. (5) is to initially apply to this program finite differences/finite elements to derive a very high-order finite-dimensional nonlinear program, and then employ reduced-basis methods (Rheinboldt, 1993; Rabier & Rheinboldt, 1995) or dual variable methods (Hall, Porsching, & Mesina, 1992; Chou & Porsching, 1998) to efficiently solve the resulting approximate program. Furthermore, modified finite difference schemes (based, for example, on Pade' approximants) have been also used to efficiently solve third- and fourth-order boundary value problems (Al-Said, Noor, & Rassias, 1998; Al-Said & Noor, 1998).

3.2. Temporal discretization

In this section, we perform temporal discretization of the dynamic nonlinear program of Eq. (8) using backward finite-differences (implicit Euler). To simplify the notation, we rewrite the program of Eq. (8) in the following form:

$$\begin{aligned}
\min \quad & \int_0^{t_f} G(a_N, d)\,\mathrm{d}t \\
\text{s.t.} \quad & \dot{a}_N = \tilde{f}(a_N, d), \\
& \tilde{g}(a_N, d) \leqslant 0,
\end{aligned} \tag{9}$$

where $a_N(t) = [a_{1N} \cdots a_{kN}]^{\mathrm{T}}$ is the vector of the time-varying coefficients of the basis eigenfunctions and the explicit form of $\tilde{f}$ and $\tilde{g}$ can be directly derived from Eq. (8). To use backward finite differences, we first discretize the temporal domain into m_t intervals and define the temporal discretization step as $\mathrm{d}t = t_f/m_t$. The vector functions $a_N(t)$ and $d(t)$ are then expressed as a series of the form

$$\begin{aligned}
a_N(t) &= \sum_{i=0}^{m_t} a_{N,i+1}[H(t - i\,\mathrm{d}t) - H((i+1)\,\mathrm{d}t - t)], \\
d(t) &= \sum_{i=0}^{m_t} d_{i+1}[H(t - i\,\mathrm{d}t) - H((i+1)\,\mathrm{d}t - t)],
\end{aligned} \tag{10}$$

where $H(\cdot)$ is the standard Heaviside function, and the time derivative at each discretization point is approximated by $\dot{a}_N(t_i) \approx \mathrm{d}t^{-1}(a_{N,i} - a_{N,i-1})$. Applying the above approximations to the dynamic nonlinear program of Eq. (9), it can be then reduced into an algebraic nonlinear program of dimension $(N + p) \times m_t$, which has the following general form:

$$\begin{aligned}
\min \quad & F(x) \\
\text{s.t.} \quad & h(x) = 0, \\
& g(x) \leqslant 0,
\end{aligned} \tag{11}$$

where the explicit form of the functions $F(x), h(x), g(x)$ is omitted for brevity.

Remark 4. Referring to the temporal discretization, we note that even though we used backward finite differences for the temporal discretization of the dynamic nonlinear program of Eq. (9) (in order to improve the numerical stability of the temporal integration), forward finite differences, as well as other temporal discretization techniques like orthogonal collocation, can be used in conjunction with the proposed spatial discretization schemes in a straightforward manner.

3.3. Computation of optimal solution

The objective of this section is to provide a computationally efficient procedure for the computation of an accurate optimal solution of the infinite-dimensional nonlinear program of Eq. (1). The central idea is to use standard reduced gradients optimization algorithms such as MINOS to solve various finite dimensional approximate programs obtained through application of the method of weighted residuals and temporal discretization using finite differences until the optimal solution is computed with the desired accuracy. The choice to employ reduced gradients optimization algorithms such as MINOS is motivated by the fact that the temporal discretization with finite-differences leads to sparse nonlinear programs for which MINOS is known to be more efficient compared to successive quadratic programming. A brief description of the MINOS algorithm is provided for completeness in Remark 5 below (see also (Biegler, Grossman, & Westerberg, 1997; Bertsekas, 1995) and the references therein for details and analysis of the algorithm). The validity of the optimal solution computed by MINOS is checked by establishing convergence to the optimum as N increases and dt decreases. We formulate the procedure used for the computation of the optimal solution of the infinite-dimensional program Eq. (5) in the form of the following algorithm:

- *Step* 1: Compute an initial guess for N, say $\hat{N}$, based on the magnitude of the eigenvalues corresponding to the eigenfunctions, and fix a dt for which a numerically stable solution of the ODE system is guaranteed.
- *Step* 2: Use the spatial and temporal discretization procedures of Sections 3.1 and 3.2, respectively, to derive a finite-dimensional program of the form of Eq. (11).
- *Step* 3: Solve the resulting finite-dimensional program using MINOS to compute an optimal solution.
- *Step* 4: Derive and solve a new finite-dimensional program of the form of Eq. (11) by performing spatial discretization with $N = \hat{N} + 1$ (dt has to be appropriately reduced).
- *Step* 5: Compare the two optimal solutions for $N = \hat{N}$ and $N = \hat{N} + 1$. If they are close (according to the desired accuracy), then stop; a convergent optimal solution has been found. If not, then go back to step 2 and perform spatial discretization with $N = \hat{N} + 2$ (again, dt has to be appropriately reduced).

The structure of the above algorithm is motivated by the fact that the discrepancy between the infinite-dimensional program and its finite-dimensional approximation of Eq. (8) decreases, as the number of basis functions, N, used in the expansion of Eq. (6) increases (at least, up to the point where round-off errors are not important). This is a consequence of the hierarchy of the eigenfunctions. On the other hand, the accuracy of the above algorithm improves as N increases and dt decreases.

Remark 5. The computation of an optimal solution of the nonlinear program of Eq. (11) with MINOS involves the solution of a sequence of subproblems with linearized constraints by using variable elimination. Specifically, the program of Eq. (11) is reformulated through the introduction of slack variables to convert the inequalities to equalities to obtain

$$\begin{aligned} \min \quad & F(x) \\ \text{s.t.} \quad & r(x) = 0. \end{aligned} \tag{12}$$

Linear approximations of the constraints are then considered with an augmented Lagrangian for the objective function:

$$\begin{aligned} \min \quad & \bar{F}(x) = F(x) + (\lambda^k)^{\mathrm{T}}[r(x) - r(x^k)] \\ \text{s.t.} \quad & J(x^k)x = b, \end{aligned} \tag{13}$$

where λ^k is the vector of Lagrange multipliers, and $J(x^k)$ is the Jacobian of $r(x)$ evaluated at the point x^k. The above problem is solved with the reduced gradient method (see, Biegler et al., 1997, for details).

Remark 6. We note that even though, for simplicity, we chose to use MINOS for solving the finite-dimensional nonlinear programs obtained from the spatial and temporal discretizations, other local (e.g., successive quadratic programming, etc.) as well as global optimization algorithms (e.g., Manousiouthakis & Sourlas, 1992; Floudas & Panos, 1992) can be used to solve the finite-dimensional programs.

Remark 7. It is important to note that while in this work we evaluate convergence of the optimization algorithms by checking the convergence of the value function as well as of the optimal input profiles (see simulation studies), one can use alternative approaches, based on derivatives of the value function within the framework of trust-region optimization, to establish convergence. In this regard, the recent works (Arian, Fahl, & Sachs, 2000; Kelley & Sachs, 1999) provide systematic approaches, based on trust-region optimization concepts, for studying global convergence of low-order approximate programs of varying accuracy to high-order optimization problems. The reader may also refer to Dennis, El-Alem, and

Maciel (1997), Alexandrov, Dennis, Lewis, and Torczon (1998), Dennis, El-Alem, and Williamson (1999), and Ulbrich, Ulbrich, and Heinkenschloss (1999) for additional results on convergence of trust-region-based optimization algorithms. In the context of using gradient-based convergence criteria, it is important to note that it is possible that higher-order approximations may be needed to obtain a convergent solution compared to the order of ones required to obtain convergence with the criteria that we employ in this work.

Remark 8. The use of global basis functions for the solution of distributed optimization lends itself nicely to procedures of sequential optimization, where the solution of an Nth-order approximation of the PDE constraints can be directly used as an initial guess for the $(N+1)$-order approximation of the PDE constraints.

3.4. Application to a diffusion-reaction process

In this subsection, we apply the optimization algorithm to a typical diffusion-reaction process with nonlinearities. Specifically, we consider a catalytic rod where an elementary exothermic reaction of the form A $\rightarrow$ B takes place. The temperature of the rod is adjusted by using one actuator located along the length of the rod. Assuming excess of species A, the spatiotemporal evolution of the dimensionless rod temperature is described by the following parabolic PDE:

$$\frac{\partial x}{\partial t} = \frac{\partial^2 x}{\partial z^2} + \beta_T \left(e^{-\gamma/(1+x)} - e^{-\gamma}\right) + \beta_U (b(z)u(t) - x) \tag{14}$$

subject to the boundary and initial conditions

$$x(0,t) = 0, \quad x(\pi,t) = 0, \quad x(z,0) = x_0(z), \tag{15}$$

where x denotes the dimensionless rod temperature, β_T denotes the dimensionless heat of reaction, γ denotes the dimensionless activation energy, β_U denotes a dimensionless heat transfer coefficient, $u(t)$ denotes the magnitude of the actuation, and $b(z)$ determines the way in which $u(t)$ is distributed along the length of the spatial domain. The nominal values of the process parameters are: $\beta_T = 8.0$, $\beta_U = 2.0$, and $\gamma = 2.0$. An accurate high-order discretization of the PDE of Eq. (14) was constructed using Galerkin's method with the following set of basis functions, derived by solving the eigenvalue–eigenfunction problem of the spatial differential operator:

$$\phi_j(z) = \sqrt{\frac{2}{\pi}} \sin(j\pi z), \quad j = 1, \ldots, \infty. \tag{16}$$

It was found that a 30th-order Galerkin truncation of the system of Eq. (14) using the above basis functions leads to an accurate solution of the PDE (it was verified that further increase in the order of the Galerkin model as well as reduction in the temporal discretization step provide no substantial improvement on the accuracy of the simulation results). Fig. 1 shows the evolution of the state of the PDE for $u(t) = 0$ starting from initial conditions which are very close to the steady state $x(z,t) = 0$. We observe that the system moves to another steady state which is characterized by a maximum at $z = 0.5$. This implies that the steady state $x(z,t) = 0$ is an unstable one, and thus, the system moves to a stable spatially non uniform steady state.

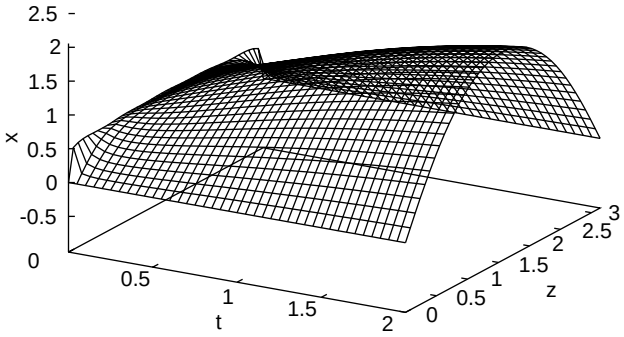

Fig. 1. Profile of the state of the PDE of Eq. (16) with $u(t) = 0$.

The operating objective of the process is to use the actuator to drive the state of the process close to the spatially-uniform steady state, $x(z,t) = 0$. To this end, we formulate the optimization problem as the one of computing an optimal input trajectory $u(t)$ for the control actuator such that a meaningful cost that includes penalty on the process response and the control action is minimized in the presence of constraints in the magnitude of the actuation. Mathematically, this optimization problem is formulated as follows:

$$\begin{aligned}
\min \quad & J = \int_0^{t_f} \int_0^1 (w_s x^2 + w_u u^2)\, dz\, dt \\
\text{s.t.} \quad & \frac{\partial x}{\partial t} = \frac{\partial^2 x}{\partial z^2} + \beta_T (e^{-\gamma/(1+x)} - e^{-\gamma}) \\
& \qquad + \beta_U (b(z)u(t) - x), \\
& x(0,t) = 0, \quad x(\pi,t) = 0, \quad x(z,0) = x_0(z), \\
& |u(t)| \leqslant M.
\end{aligned}$$

The nominal values of the process and optimization parameters were taken as: $x_0(z) = 0.5$, $M = 0.6$, $b(z) = H(z - 0.3\pi) - H(z - 0.7\pi)$, where H denotes the standard Heaviside function, $w_s = 100$ and $w_u = 20$.

We computed an optimal solution to the above problem by performing spatial discretization using Galerkin's method with the eigenfunctions of Eq. (16) as basis functions and temporal discretization using implicit Euler to ensure numerical stability of the temporal integration. The resulting nonlinear program was solved with MINOS. Optimal solution profiles for $u(t)$ were computed for different numbers of basis functions (in all these cases the step of the temporal discretization was appropriately adjusted to guarantee numerical stability of the temporal integration) to obtain a convergent solution profile. Fig. 2 shows the profiles of $u(t)$

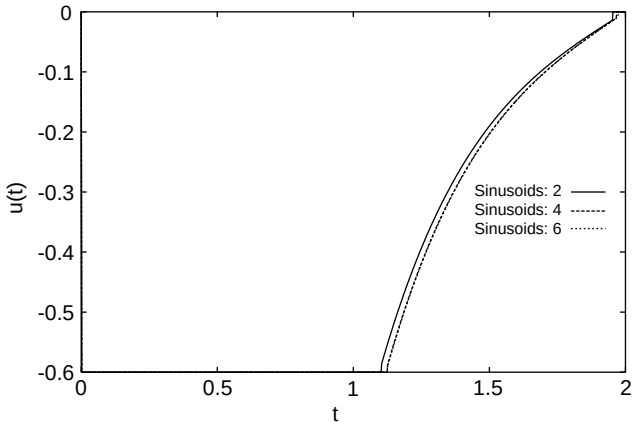

Fig. 2. Profiles of $u(t)$ for $N = 2, 4, 6$ for nominal values of the process parameters—convergence to an optimal $u(t)$.

for different number of global basis functions, $N = 2, 4, 6$, which clearly converge to an optimal profile, for $N = 6$; note that the resulting $u(t)$ satisfies the constraint, $|u(t)| \leqslant 0.6$, for all times. Fig. 3 shows the profile of the state $x(z, t)$ for $N = 6$; it is clear that the optimal input profile helps driving the state of the PDE system close to the spatially uniform steady state at a finite time, which is consistent with the requested optimization objective. The speed of the transient response of the process towards the spatially uniform steady state depends heavily on the relationship between the weights, w_s and w_u used in the objective function, the system state gets closer to $x(z, t) = 0$, when less weight is placed on the input $u(t)$ (this is expected since the control action is penalized less in such a case).

As a numerical note, we point out that, in addition to computing a convergent optimal solution profile, the time needed to solve the optimization problem was about 25 min which is a very small fraction of the time needed to solve this problem, with the same degree of accuracy, when spatial discretization is performed using the centered *finite—difference* method; this is consistent with similar comparisons made for steady-state optimization problems with PDE constraints (Bendersky & Christofides, 2000). We also note that the time needed to solve the optimization problem increased considerably with the order of the approximation of the PDE as can be seen in the results presented in Table 1.

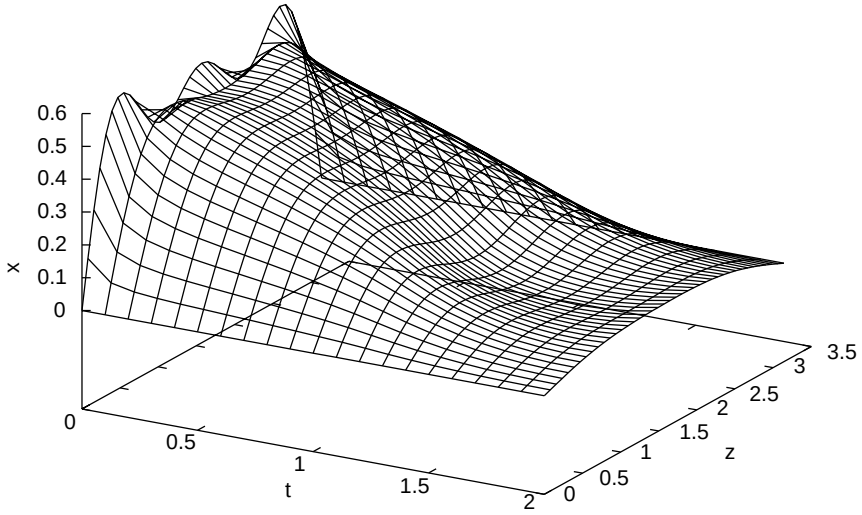

Fig. 3. Profile of the state of the PDE of Eq. (16) for optimal $u(t)$ ($N = 6$).

Table 1
Optimization results for diffusion-reaction process with constant parameters

Number of basis functions	Process parameters	Design variables	Objective	Time	Fig.
1	Nominal	1	22.453986	418.7	2
2	Nominal	1	22.455112	557.2	2
3	Nominal	1	23.630877	705.0	2
4	Nominal	1	23.630829	919.9	2
6	Nominal	1	23.687086	1506.0	2
6	-12.5% β_T	1	13.632773	1699.1	4
6	-20% x_0	1	11.745360	1608.8	6
6	$b(\zeta) = H(\zeta - 0.01) - H(\zeta - 0.4)$	1	89.554427	1152.8	8
6	Nominal	2	47.483544	2649.9	10
6	-12.5% β_T	2	23.451269	3530.4	13

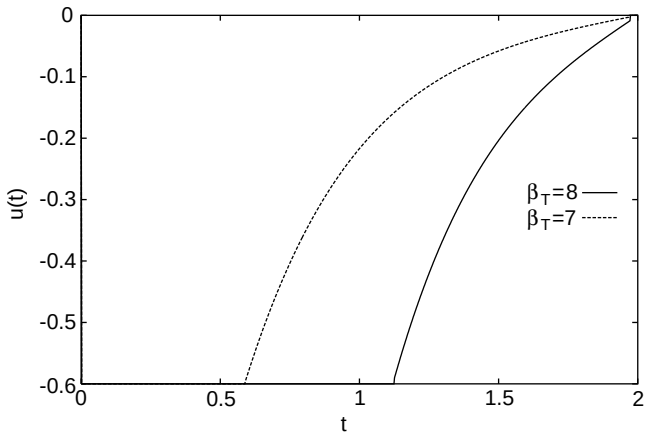

Fig. 4. Optimal solution profiles for nominal parameters and for a 12.5% variation in β_T.

To test the robustness of the optimization approach and evaluate the degree of convergence to the optimal $u(t)$, we solved several optimization problems obtained by varying the process parameters, initial conditions and actuator distribution functions. Fig. 4 shows the convergent profile of $u(t)$ $(N=6)$ for a -12.5% variation in β_T and Fig. 5 shows the corresponding profile of the state $x(z,t)$. Fig. 6 shows the convergent profile of $u(t)$ $(N=6)$ and Fig. 7 shows the corresponding profile of the state $x(z,t)$ for a -20% variation in the initial condition; the optimal input profiles lead to operation of the process close to the spatially uniform steady-state at a finite time. In both cases the system is driven to the spatially uniform steady state faster and with less control action, since in the first case the effect of the destabilizing nonlinearity is smaller and in the second case the system starts closer to the spatially uniform steady state.

Moreover, for the nominal set of process parameters and for $x_0(z)=0.5$, we solved the nonlinear program using the proposed approach for two different choices of actuator distribution functions and number of actuators. First, the position of the actuator was shifted to the left of the center of the catalytic rod, i.e., $b(z)=H(z-0.01\pi)-H(z-0.4\pi)$. Fig. 8 shows the convergent profile of $u(t)$ $(N=6)$ and Fig. 9 shows the corresponding profile of the state $x(z,t)$. As expected, in the new position the actuator is less effective on the system than in the original one (note that the constraint on the control action, M, remains the same), and as a result the optimal control action stays longer on the bounds. We also observe in Fig. 9 that the actuator fails to efficiently drive the system to the spatially uniform steady state, with the left side of the system being close to zero and the right side away from zero.

Finally, we considered the case of achieving the process operating objective by using two actuators with $b_1=H(z-0.2\pi)-H(z-0.4\pi)$ and $b_2=H(z-0.6\pi)-H(z-0.8\pi)$. The spatial interval in which each individual actuator acts is the same, and the actuators are placed at symmetrical positions relative to the center of the spatial domain. In Fig. 10 we present the profiles of $u_1(t)$ and $u_2(t)$ and compare them to the nominal case. We observe that the action of the two actuators is the same, an expected result due to the symmetry of the system around the center of the catalytic rod. Fig. 11 presents the spatiotemporal profile of $x(z,t)$ where we observe the effect that the two actuators have on the system. Note that the system is not driven to the spatially uniform steady state as effectively as in the nominal case, due to the fact that the actuators are not placed at the center of the catalytic rod (where the effect of the actuator on the system is maximal). For the case of two actuators, we also

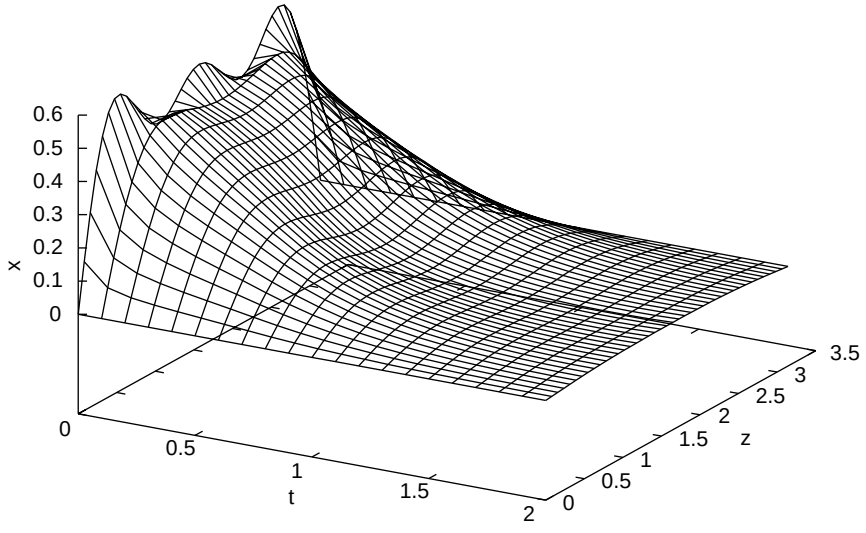

Fig. 5. State profile for optimal $u(t)$—12.5% variation in β_T.

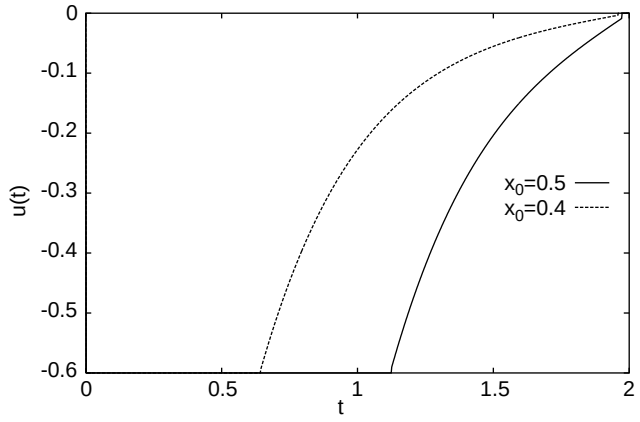

Fig. 6. Optimal solution profiles for nominal parameters and for a −20% variation of the initial condition ($x_0 = 0.4$).

solved the nonlinear program for the value of $\beta_T = 7$ (reduced effect of the destabilizing nonlinear terms on the system). We see that for this case the use of two control actuators is sufficient to drive the system close to the spatially uniform steady-state, shown in Fig. 12; the optimal profiles of $u(t)$ are shown in Fig. 13.

4. Spatial discretization using global empirical eigenfunctions

4.1. Computation of empirical eigenfunctions via Karhunen–Loève expansion

In this section, we use of solution data of the system of Eq. (1) to construct global basis functions using Karhunen–Loève (K–L) expansion. The motivation for studying this approach is provided by the occurrence of dominant spatial patterns in the solution of several dissipative PDEs, which should be accounted for in the shape of the global basis functions. This approach will be useful in the context of systems of dissipative PDEs that involve nonlinear spatial differential operators and spatially-varying coefficients that lead to non-symmetric solution profiles (see the example in the next subsection). K–L is a procedure used to compute an optimal (in a sense that will become clear below) set of empirical eigenfunctions from an appropriately constructed set of solutions of the PDE system of Eq. (1) obtained from high-order discretization. In this work, the ensemble of solutions is constructed by computing the solutions of the PDE system of Eq. (1) for different profiles of $d(t)$, and different initial conditions. Specifically, we construct a representative ensemble using the following procedure (see also Graham & Kevrekidis, 1996; Bendersky & Christofides, 2000 for more discussion on ensemble construction):

- First, we create a set of different initial conditions.
- We then discretize the interval in which each design variable d_m ($m = 1, \ldots, p$) is constrained to be into m_{d_m} (not necessarily equispaced) subintervals. The discrete values of d_m are denoted by $d_{m,j}$, $j = 1, \ldots, m_{d_m}$.
- We also discretize the time interval into n_{d_m} time subintervals (also not necessarily equispaced).
- Subsequently, we compute a set of time profiles for each of the design variables $d_m(t)$ by assigning values for $d_m(t)$ at different time instants t_j, say $d_{m,j}$, and subsequently computing $d_m(t)$ for the entire time interval of process operation using linear interpolation.
- Finally, we compute a set of PDE solution data (ensemble) for all possible combinations of initial conditions and profiles of $d(t)$.

Application of K–L expansion to this ensemble of data provides an orthogonal set of basis functions (known as

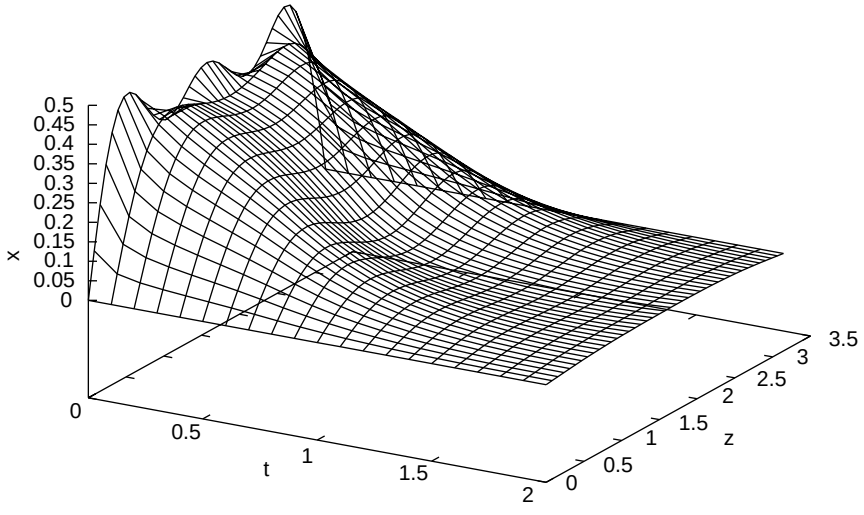

Fig. 7. State profile for optimal $u(t)$: −20% variation of the initial condition ($x_0 = 0.4$).

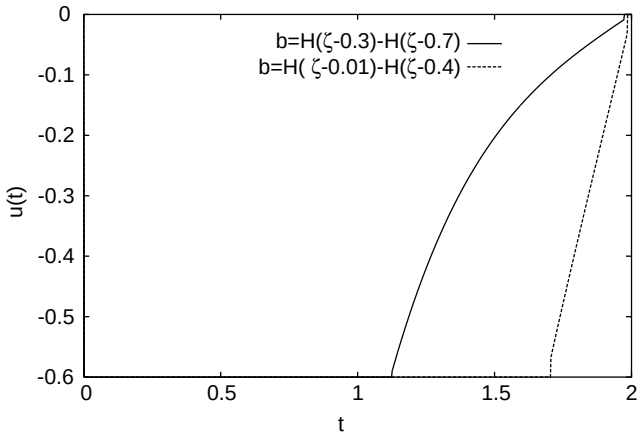

Fig. 8. Optimal solution profiles for nominal parameters and for a new actuator distribution function $b(\zeta) = H(\zeta - 0.01) - H(\zeta - 0.4)$, $\zeta \in [0, 1]$.

empirical eigenfunctions) for the representation of the ensemble, as well as a measure of the relative contribution of each basis function to the total energy (mean square fluctuation) of the ensemble. A truncated series representation of the ensemble data in terms of the dominant basis functions has a smaller mean square error than a representation by any other basis of the same dimension (Holmes, Lumley, & Berkooz, 1996). This implies that the projection on the subspace spanned by the empirical eigenfunctions will on average contain the most energy possible compared to all other linear decompositions, for any number of modes L. Therefore, the K–L expansion yields the most efficient way for computing the basis functions (corresponding to the largest empirical eigenvalues) capturing the dominant patterns of the ensemble.

For simplicity of the presentation, we describe the K–L expansion in the context of the system of Eq. (1) with $n = 1$ and assume that there is available a sufficiently large set of solutions of this system for different values of d, $\{\bar{v}_\kappa\}$, consisting of K sampled states, $\bar{v}_\kappa(z)$, (which are typically called "snapshots"). We assume that the snapshots are linearly independent; the reader may refer to Fukunaga (1990) and Holmes et al. (1996) for a detailed presentation and analysis of the K–L expansion. We define the ensemble average of snapshots as $\langle \bar{v}_\kappa \rangle := (1/K) \sum_{\kappa=1}^{K} \bar{v}_\kappa(z)$ (we note that nonuniform sampling of the snapshots and weighted ensemble average can be also considered; see, for example, Graham & Kevrekidis, 1996). Furthermore, the ensemble average of snapshots $\langle \bar{v}_\kappa \rangle$ is subtracted out from the snapshots, i.e.

$$v_\kappa = \bar{v}_\kappa - \langle \bar{v}_\kappa \rangle \tag{17}$$

so that only fluctuations are analyzed. The issue is how to obtain the most typical or characteristic structure (in a sense that will become clear below) $\phi(z)$ among these snapshots $\{v_\kappa\}$. Mathematically, this problem can be posed as the one of obtaining a function $\phi(z)$ that maximizes the following objective function:

$$\begin{aligned} &\max. \quad \frac{\langle (\phi, v_\kappa)^2 \rangle}{(\phi, \phi)} \\ &\text{s.t.} \quad (\phi, \phi) = 1, \quad \phi \in L^2([\Omega]). \end{aligned} \tag{18}$$

The constraint $(\phi, \phi) = 1$ is imposed to ensure that the function, $\phi(z)$, computed as a solution of the above maximization problem, is unique. The Lagrangian functional corresponding to this constrained optimization problem is

$$\bar{L} = \langle (\phi, v_\kappa)^2 \rangle - \lambda((\phi, \phi) - 1) \tag{19}$$

and necessary conditions for extrema is that the functional derivative vanishes for all variations $\phi + \delta\psi \in L^2[\Omega]$, where δ is a real number:

$$\frac{d\bar{L}(\phi + \delta\psi)}{d\delta}(\delta = 0) = 0, \quad (\phi, \phi) = 1. \tag{20}$$

Using the definitions of inner product and ensemble average, $(d\bar{L}(\phi+\delta\psi)/d\delta)(\delta=0)$ can be computed from the following

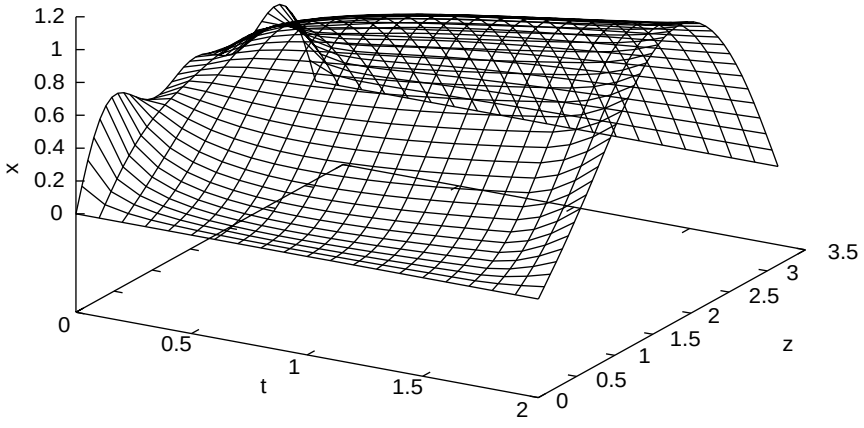

Fig. 9. State profile for optimal $u(t) - b(\zeta) = H(\zeta - 0.01) - H(\zeta - 0.4)$, $\zeta \in [0, 1]$.

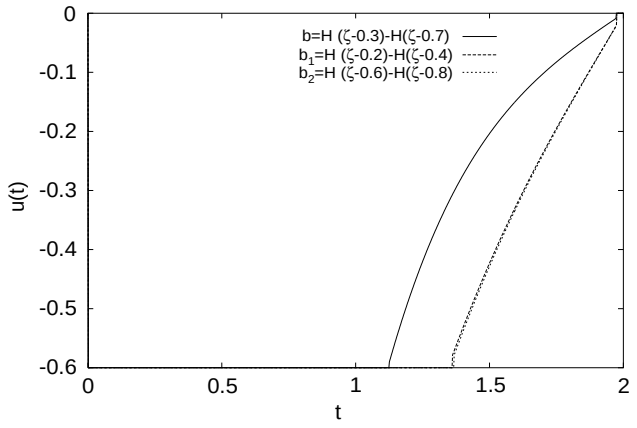

Fig. 10. Optimal solution profiles for nominal case and for the case of using two control actuators with $b_1(\zeta) = H(\zeta - 0.2) - H(\zeta - 0.4)$, $b_2(\zeta) = H(\zeta - 0.6) - H(\zeta - 0.8)$, $\zeta \in [0, 1]$.

expression:

$$\frac{\mathrm{d}\bar{L}(\phi + \delta\psi)}{\mathrm{d}\delta}(\delta = 0) = \int_\Omega \left(\left\{ \int_\Omega \langle v_\kappa(z) v_\kappa(\bar{z}) \rangle \phi(z)\, \mathrm{d}z \right\} - \lambda\phi(\bar{z}) \right) \psi(\bar{z})\, \mathrm{d}\bar{z}. \tag{21}$$

Since $\psi(\bar{z})$ is an arbitrary function, the necessary conditions for optimality take the form

$$\int_\Omega \langle v_\kappa(z) v_\kappa(\bar{z}) \rangle \phi(z)\, \mathrm{d}z = \lambda\phi(\bar{z}), \quad (\phi, \phi) = 1. \tag{22}$$

Introducing the two-point correlation function

$$K(z, \bar{z}) = \langle v_\kappa(z) v_\kappa(\bar{z}) \rangle = \frac{1}{K} \sum_{\kappa=1}^{K} v_\kappa(z) v_\kappa(\bar{z}) \tag{23}$$

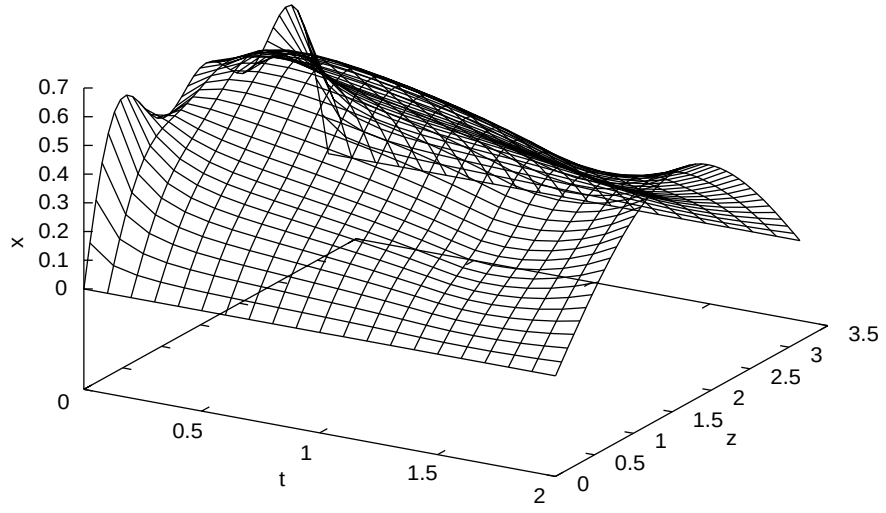

Fig. 11. State profile for optimal $u(t)$—two control actuators.

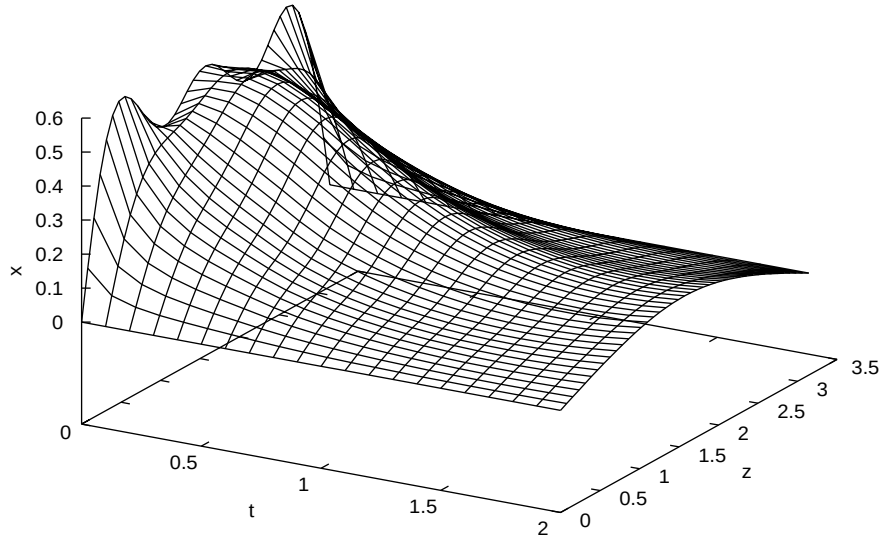

Fig. 12. State profile for optimal $u(t)$—two control actuators and $\beta_t = 7$.

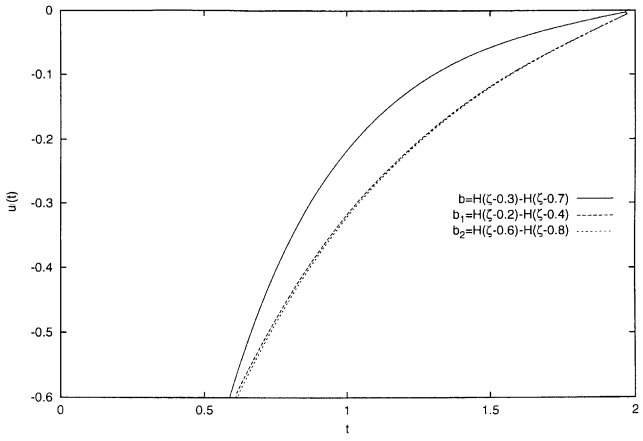

Fig. 13. Optimal solution profiles for $\beta_t = 7$ and for two control actuators with $b_1(\zeta) = H(\zeta - 0.2) - H(\zeta - 0.4)$, $b_2(\zeta) = H(\zeta - 0.6) - H(\zeta - 0.8)$, $\zeta \in [0, 1]$.

and the linear operator

$$R := \int_\Omega K(z, \bar{z})\, \mathrm{d}\bar{z} \tag{24}$$

the optimality condition of Eq. (22) reduces to the following eigenvalue problem of the integral equation:

$$R\phi = \lambda\phi \Rightarrow \int_\Omega K(z, \bar{z})\phi(\bar{z})\, \mathrm{d}\bar{z} = \lambda\phi(z). \tag{25}$$

The computation of the solution of the above integral eigenvalue problem is, in general, a very expensive computational task. To circumvent this problem, Sirovich introduced in 1987 (Sirovich, 1987a, b) the method of snapshots. The central idea of this technique is to assume that the requisite eigenfunction, $\phi(z)$, can be expressed as a linear combination of the snapshots, i.e.,

$$\phi(z) = \sum_k c_k v_k(z). \tag{26}$$

Substituting the above expression for $\phi(z)$ on Eq. (25), we obtain the following eigenvalue problem:

$$\int_\Omega \frac{1}{K} \sum_{\kappa=1}^{K} v_\kappa(z) v_\kappa(\bar{z}) \sum_{k=1}^{K} c_k v_k(\bar{z})\, \mathrm{d}\bar{z} = \lambda \sum_{k=1}^{K} c_k v_k(z). \tag{27}$$

Defining

$$B^{\kappa k} := \frac{1}{K} \int_\Omega v_\kappa(\bar{z}) v_k(\bar{z})\, \mathrm{d}\bar{z} \tag{28}$$

the eigenvalue problem of Eq. (27) can be equivalently written as

$$Bc = \lambda c. \tag{29}$$

The solution of the above eigenvalue problem (which can be obtained by utilizing standard methods from matrix theory) yields the eigenvectors $c = [c_1 \cdots c_K]$ which can be used in Eq. (26) to construct the eigenfunction $\phi(z)$. From the structure of the matrix B, it follows that is symmetric and positive semi-definite, and thus, its eigenvalues, λ_κ, $\kappa = 1, \ldots, K$, are real and non-negative. Furthermore, the resulting eigenfunctions form an orthogonal set, i.e.:

$$\int_\Omega \phi_i(z)\phi_j(z)\, \mathrm{d}z = 0, \quad i \neq j. \tag{30}$$

The solution of the optimization program of Eq. (5) using a set of empirical eigenfunctions as global basis functions in the method of weighted residuals is similar to the approach described in the previous section, and therefore, it will not be repeated. Instead, a numerical example of a dynamic optimization problem for a diffusion-reaction process with spatially varying coefficients will be presented in the next subsection.

Remark 9. In the context of transport-reaction process optimization few papers have appeared in the literature that utilize the method of weighted residuals with empirical eigenfunctions obtained through K–L expansion as the means of solving infinite-dimensional nonlinear programs. A notable exception is the recent paper (Park & Lee, 1998) where an ill-posed inverse heat convection problem was efficiently discretized using Galerkin's method with empirical eigenfunctions and solved through conjugate gradient method.

Remark 10. We note that the basis that we compute using K–L decomposition is independent of the functional that we try to minimize. Therefore, the same basis can be used to perform computationally efficient optimizations with respect to different functionals associated with the same underlying set of partial differential equations.

Remark 11. We note that the value of m_{d_m} should be determined based on the effect of the design variable d_m on the solution of the system of Eq. (1) (if, for example, the effect of the variable d_1 is larger that the effect of the variable d_2, then m_{d_1} should be larger than m_{d_2}).

Remark 12. As a practical implementation note, we point out that even though it is expected that the use of more basis functions in the series expansion of Eq. (6) would improve the accuracy of the computed approximate model of Eq. (8), the use of empirical eigenfunctions corresponding to very small eigenvalues should be avoided because such eigenfunctions are contaminated with significant round-off errors.

4.2. Application to a diffusion-reaction process with nonlinear spatial operator and a spatially varying coefficient

We consider the diffusion-reaction process of Section 3.4 and assume that the spatial differential operator is nonlinear (e.g., nonlinear dependence of the thermal conductivity on

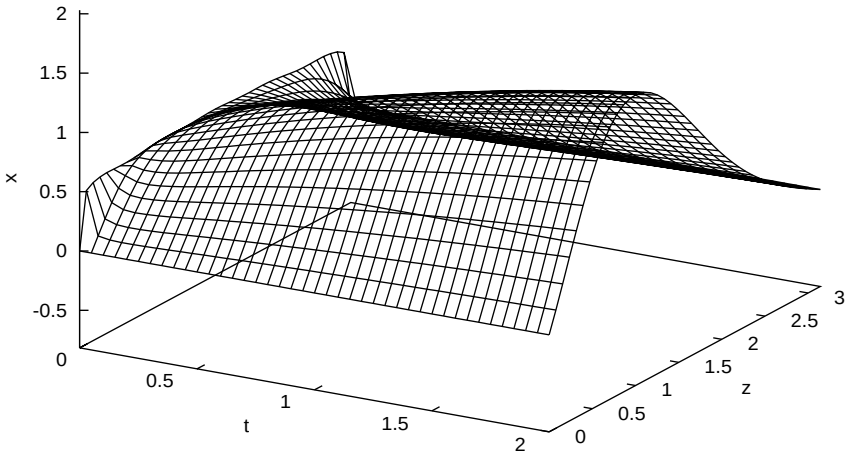

Fig. 14. Profile of the state of the PDE of Eq. (32) with $u(t) = 0$.

temperature) and that the dimensionless reaction rate can stand β_T is spatially-varying. In this case, the process model is given by the following nonlinear parabolic PDE:

$$\frac{\partial x}{\partial t} = \frac{\partial x}{\partial z}\left(k(x)\frac{\partial x}{\partial z}\right) + \beta_T(z)(e^{-\gamma/(1+x)} - e^{-\gamma}) + \beta_U(b(z)u(t) - x) \tag{31}$$

subject to the Dirichlet boundary conditions

$$x(0,t) = 0, \quad x(\pi,t) = 0 \tag{32}$$

and the initial condition

$$x(z,0) = x_0(z), \tag{33}$$

where x is the state of the system, $k(x)$ is an explicit nonlinear function of the state, γ, β_u are constant dimensionless process parameters, $\beta_T(z)$ is a dimensionless process parameter that is an explicit function of the spatial coordinate z, $u(t)$ is the magnitude of the actuation and $b(z)$ is the actuator distribution function. The nominal values and expressions of the process parameters that were used in our calculations are: $x_0(z) = 0.5$, $k = 0.5 + 0.7/(x+1)$, $\beta_T = 12[\cos(z) + 1]$, $\beta_u = 2.0$, $\gamma = 2.0$, and $b(z) = H(z - 0.1\pi) - H(z - 0.5\pi)$. For these values, the operating steady-state $x(z,t) = 0$ is an unstable one, and the system converges to a stable nonuniform steady state (as can be seen in Fig. 14 for an initial condition of $x_0(z) = 0.5$). As a result, the optimization problem is formulated as the one of computing an optimal input trajectory $u(t)$ for the control actuator such that a meaningful cost that includes penalty on the process response and the control action is minimized in the presence of constraints in the magnitude of the actuator. Mathematically, this optimization problem is formulated as follows:

$$\min J = \int_0^{t_f}\int_0^1 (w_s x^2 + w_u u^2)\,dz\,dt$$

$$\frac{\partial x}{\partial t} = \frac{\partial x}{\partial z}\left(k(x)\frac{\partial x}{\partial z}\right) + \beta_T(z)(e^{-\gamma/(1+x)} - e^{-\gamma}) + \beta_U(b(z)u(t) - x)$$

$$x(0,t) = 0, \quad x(\pi,t) = 0, \quad x(z,0) = x_0(z)$$

$$|u(t)| \leqslant M, \tag{34}$$

where $M = 0.6$, $w_s = 100$ and $w_u = 20$. Initially, we computed an optimal solution to the above problem by performing spatial discretization using Galerkin's method with the sinusoidal functions of Eq. (16) as basis functions and temporal discretization using Euler's implicit method. The resulting nonlinear program was solved with MINOS. Optimal solution profiles for $u(t)$ were computed for different numbers of basis functions (in all these cases the step of the temporal discretization was appropriately adjusted to guarantee numerical stability of the temporal integration) to obtain a convergent solution profile. Fig. 15 (top plot) shows the resulting profiles of $u(t)$ for $N = 2, 3, 4$ which clearly converge to a single optimal profile, for $N = 4$; note that $u(t)$ satisfies $|u(t)| \leqslant 0.6$. Fig. 15 (bottom plot) shows the profile of the state $x(z,t)$ for optimal $u(t)$ for $N = 4$; it is clear that the optimal input profile leads to operation of the process close to the spatially uniform steady state at a finite time. The time to converge to the optimal solution depends strongly on the order of the discretization and is presented in Table 2. Specifically, the time to solve the problem for a fourth order discretization of the system is 1156.0 s, which is again a fraction of the time needed to solve the program of Eq. (34) using finite-differences for spatial discretization.

We now proceed with the solution of the nonlinear program of Eq. (34) by performing spatial discretization using Galerkin's method with empirical eigenfunctions as basis functions. In order to evaluate the effect of the construction of the ensemble on the performance of the

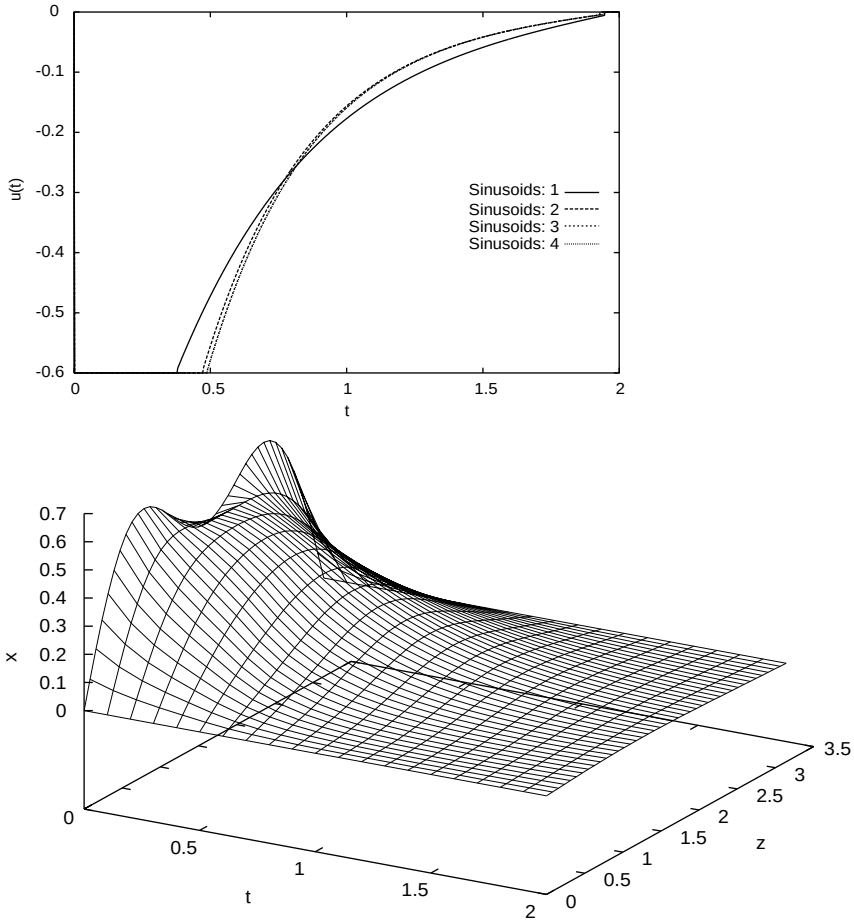

Fig. 15. (Top plot) Profiles of $u(t)$ in the case of using sinusoids as basis functions. (Bottom plot) Profile of the state of the PDE of Eq. (32) for optimal $u(t)$ ($N = 4$).

optimization methods, we constructed two different ensembles and used them to solve the optimization problem of Eq. (34).

First, we derived and solved a high-order and convergent discretization of the PDE of Eq. (31) for $x_0 = 0.5$ and $x_0 = 0.0$, and for several different and arbitrary variations of the input $u(t)$, using a distribution function of the form $b(\zeta) = H(\zeta - 0.1) - H(\zeta - 0.5)$ ($\zeta = z/l$, $l = \pi$ is the length of the domain). From this set of simulations, we computed a total of eight spatiotemporal solution profiles. Subsequently, 37 "snapshots" were taken from each solution data set and were combined, to generate an ensemble of 296 solutions. The Karhunen–Loève expansion was then applied to the developed ensemble of solutions to compute seven empirical eigenfunctions that describe the dominant spatial solution patterns embedded in the ensemble (they account for more than 99.99% of the energy included in the entire ensemble). The first three of these empirical eigenfunctions are presented in Fig. 16. Note that in contrast to the sinusoidal functions, these eigenfunctions are not symmetric with respect to the center of the spatial domain, owing to the spatial non-uniformity of the term $\beta_T = 12[\cos(z) + 1]$, and its coupling with the nonlinearity $k(x) = 0.7/(x + 1) + 0.5$.

Furthermore, we computed a second set of empirical eigenfunctions by using three control actuators with $b_1(z) = 1$, $b_2 = H(z - 0.1\pi) - H(z - 0.5\pi)$ and $b_3(z) = \delta(z - 0.3\pi)$, and arbitrary time-varying inputs, as well as two different initial conditions $x_0 = 0.5$ and $x_0 = 0.0$. An ensemble of 1554 solutions was constructed. The Karhunen–Loève expansion was then applied to the developed ensemble of solutions to compute nine empirical eigenfunctions that describe the dominant spatial solution patterns embedded in the ensemble (they account for more than 99.99% of the energy included in the entire ensemble). The first three of these empirical eigenfunctions are presented in Fig. 17. Note that they are not symmetric with respect to the center of the system, $z = 0.5\pi$, owing to the spatial non-uniformity of $\beta_T = 12[\cos(z) + 1]$ and the nonlinearity $k = 0.7/(x + 1) + 0.5$ and furthermore that they capture the effect that the point control actuator has on the state of the system.

We initially computed an optimal solution to the problem of Eq. (34) by performing spatial discretization using Galerkin's method with the first set of empirical eigenfunctions as basis functions and temporal discretization using Euler's implicit method. The resulting nonlinear program was

Table 2
Optimization results for diffusion-reaction process with nonlinear spatial differential operator and spatially varying parameters

Number/type of basis functions	Process parameters	Design variables	Objective	Time (s)	Fig.
1/Emp. Set 1	Nominal	1	11.0401	599.6	18a
2/Emp. Set 1	Nominal	1	11.1583	747.2	18a
3/Emp. Set 1	Nominal	1	11.7786	935.2	18a
1/Sinusoid	Nominal	1	11.1431	639.8	15a
2/Sinusoid	Nominal	1	11.3400	747.3	15a
3/Sinusoid	Nominal	1	11.7805	935.8	15a
4/Sinusoid	Nominal	1	11.8013	1156.0	15a
1/Emp. Set 2	Nominal	1	11.5275	603.5	19a
2/Emp. Set 2	Nominal	1	11.6023	747.6	19a
3/Emp. Set 2	Nominal	1	11.7203	935.2	19a
3/Emp. Set 1	-20% x_0	1	7.0274	960.1	22a
4/Sinusoid	-20% x_0	1	7.0511	1191.7	
3/Emp. Set 1	$k(x) = 1.0$	1	12.6741	960.1	21a
3/Sinusoid	$k(x) = 1.0$	1	12.6211	955.8	
4/Sinusoid	$k(x) = 1.0$	1	12.6582	1186.2	
3/Emp. Set 1	-12.5% β_T	1	8.3823	1014.1	20a
3/Sinusoid	-12.5% β_T	1	8.3942	1249.4	
3/Emp. Set 1	Nominal	1	14.7365	899.3	23a
3/Emp. Set 1	Nominal	2	27.2674	1874.3	24a
4/Sinusoid	Nominal	2	26.6595	2288.1	
5/Sinusoid	Nominal	2	27.1428	2703.8	
2/Emp. Set 2	Nominal	2	4.5373	2517.0	25a,b
3/Emp. Set 2	Nominal	2	4.6918	2654.6	25a,b
5/Emp. Set 2	Nominal	2	4.7215	2714.3	25a,b
3/Sinusoid	Nominal	2	4.3459	2708.6	26a,b
4/Sinusoid	Nominal	2	4.3816	3273.0	26a,b
5/Sinusoid	Nominal	2	4.4615	3973.5	26a,b
6/Sinusoid	Nominal	2	4.4695	4847.8	26a,b
9/Sinusoid	Nominal	2	4.4829	9891.0	

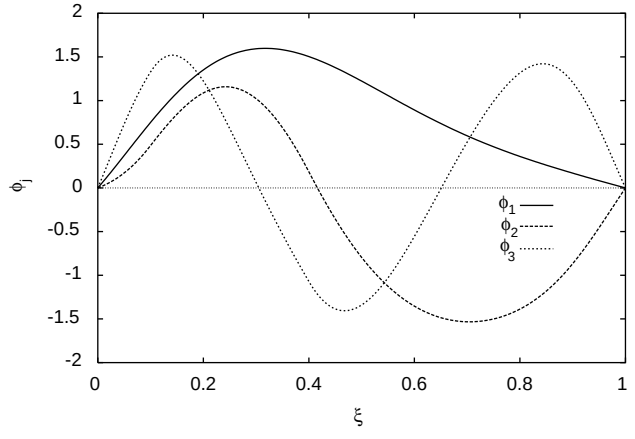

Fig. 16. First three empirical eigenfunctions for single actuator with $b(\zeta) = H(\zeta - 0.1) - H(\zeta - 0.5)$.

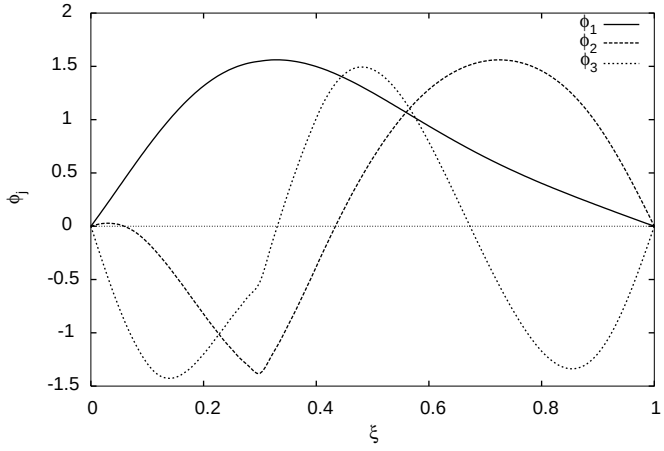

Fig. 17. First three empirical eigenfunctions for ensemble constructed by using three control actuators.

solved with MINOS. Optimal solution profiles for $u(t)$ were computed for different numbers of empirical eigenfunctions to obtain a convergent solution profile. Fig. 18 (top plot) shows the profiles of $u(t)$ for $N = 1, 2, 3$ which clearly converge to a single profile, for $N = 3$; note that $u(t)$ satisfies the imposed constraints. Fig. 18 (bottom plot) shows the profile of the state $x(z, t)$ for $N = 3$; it is clear that the optimal input profile leads to operation of the process close to the spatially uniform steady state at a finite time. Furthermore, the time needed to solve the optimization problem was 935.2 s which is a small fraction of the time needed to solve this problem, with the same degree of accuracy, when spatial discretization is performed using finite differences. We also solved the problem of Eq. (34) by performing spatial discretization

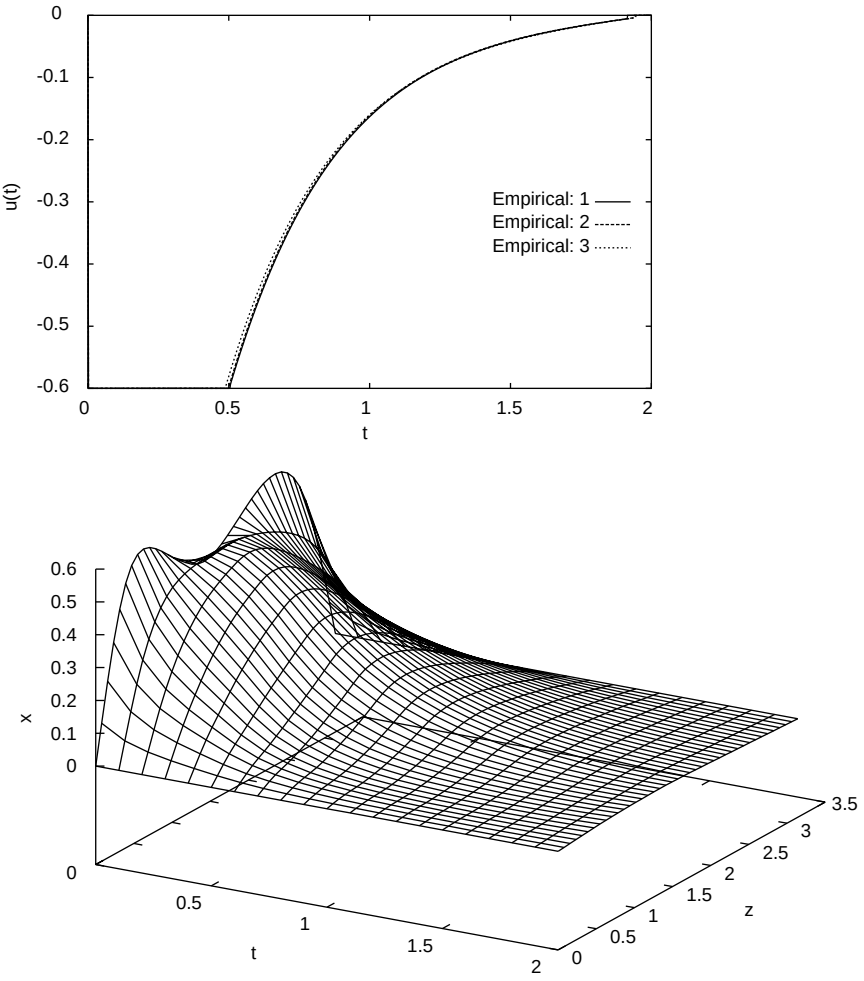

Fig. 18. (Top plot) Profiles of $u(t)$ in the case of using the first set of empirical eigenfunctions as basis functions. (Bottom plot) Profile of the state of the PDE of Eq. (32) for optimal $u(t)$ ($N = 3$).

using Galerkin's method with the second set of empirical eigenfunctions as basis functions. The results are shown in Fig. 19. Clearly, the use of the second set of eigenfunctions leads to an efficient solution of the optimization problem; an important advantage of the second set of eigenfunctions (which accounts for the effect of the point actuator on the system solution) will be discussed below (see Figs. 25 and 26).

We also used the first set of eigenfunctions to compute the solution of the optimization problem of Eq. (34) when different process parameters and initial conditions are used. Fig. 20 shows the convergent profile of $u(t)$ ($N = 3$) for a 12.5% variation in β_T and the corresponding profile of the state $x(z,t)$, Fig. 21 shows the convergent profile of $u(t)$ ($N = 3$) when $k = 1.0$, and Fig. 22 shows the convergent profile of $u(t)$ ($N = 3$) and the corresponding profile of the state $x(z,t)$ for a 20% variation in the initial condition; again the optimal input profiles lead to operation of the process close to the spatially uniform steady state at a finite time.

Moreover, for the nominal set of process parameters and the initial condition, we solved the nonlinear program of Eq. (34) for two different choices of actuator distribution functions. First, the position of the actuator was shifted to the right of the center of the catalytic rod, i.e., $b(z) = H(z - 0.3\pi) - H(z - 0.7\pi)$. Fig. 23 (top plot) shows the convergent profile of $u(t)$ ($N = 3$) and Fig. 23 (bottom plot) shows the corresponding profile of the state $x(z,t)$. As expected (see also discussion in the first example), in the new position the actuator is less effective on the system, and as a result the optimal control action is one that stays longer on the bounds. We also observe in Fig. 23b that the actuator fails to completely drive the state of the system to the spatially uniform steady state. Furthermore, we considered the case of using two actuators with $b_1(z) = H(z - 0.01\pi) - H(z - 0.2\pi)$ and $b_2(z) = H(z - 0.4\pi) - H(z - 0.6\pi)$. The two actuators influence spatial intervals of the same size and are symmetrically placed with respect to the maximum value of the state of the system (see Fig. 14). Fig. 24 (top plot) presents the profiles of $u_1(t)$ and $u_2(t)$ and compares them to the nominal case. We observe that the action of the two actuators is different, contrary to the case of constant process parameters; this is expected since the system is lacking symmetry around the

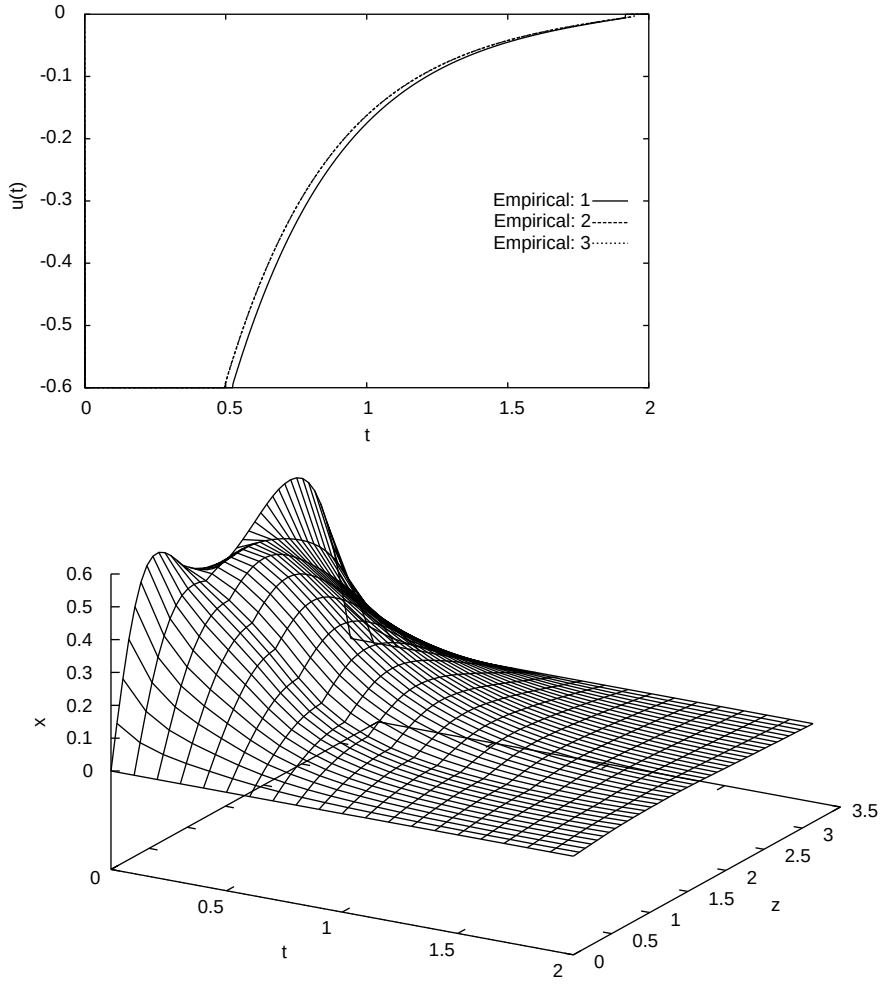

Fig. 19. (Top plot) Profiles of $u(t)$ in the case of using the second set of empirical eigenfunctions as basis functions. (Bottom plot) Profile of the state of the PDE of Eq. (32) for optimal $u(t)$ ($N = 3$).

point of maximum temperature of the catalytic rod. Fig. 24 (bottom plot) presents the spatiotemporal profile of $x(z,t)$ where we observe the effect that the two actuators have on the system. Note that the system is not driven to the spatially uniform steady state as effectively as in the nominal case, due to the fact that the actuators are not placed at the position of maximum effect on the state of the system.

Finally, for the nominal set of process parameters and the initial condition, we solved the nonlinear program of Eq. (34) in the case of using two control actuators with $b_1(z) = H(z - 0.1\pi) - H(z - 0.5\pi)$ ($w_{u_1} = 25$) and $b_2(z) = \delta(z - 0.3\pi)$ (point control actuation; $w_{u_2} = 15$). In this case, the bound on the available control action was taken to be $M = 0.4$. The second set of empirical eigenfunctions were used as basis functions since they were constructed by using an ensemble which includes solutions obtained by applying point control actuation to the PDE. Fig. 25a (top plots) show the convergent profiles of $u_1(t)$ and $u_2(t)$ for $N = 2, 3$ and Fig. 25b (bottom plot) shows the corresponding profile of the state $x(z,t)$ for $N = 3$. For comparison purposes, the same optimization problem was solved using sinusoid basis functions. Fig. 26 presents the profiles $u_1(t)$ and $u_2(t)$ for $N = 3, 4, 5, 6$. We observe that the optimization algorithm that uses sinusoid basis functions converges to the solution computed using three empirical eigenfunctions very slowly. This is due to the fact that the empirical eigenfunctions capture efficiently the effect the point actuator has on the state of the system, while the sinusoidal basis functions do not account for this effect. This result shows the usefulness of using basis functions constructed from appropriate solution data (in the sense that they capture the effect of the actuators) versus an off-the-shelf set of basis functions. From Table 2, we see that the total time to solve the program of Eq. (34) in this case, using empirical eigenfunctions, was much smaller than the time needed to solve this program using a larger number ($N = 6, 9$) of sinusoidal basis functions.

Remark 13. We note that the time needed to compute the empirical eigenfunctions was not included in the calculation of the time (Table 2) needed to solve the optimization problem through empirical eigenfunction-based Galerkin method. The reason is that the computed sets of

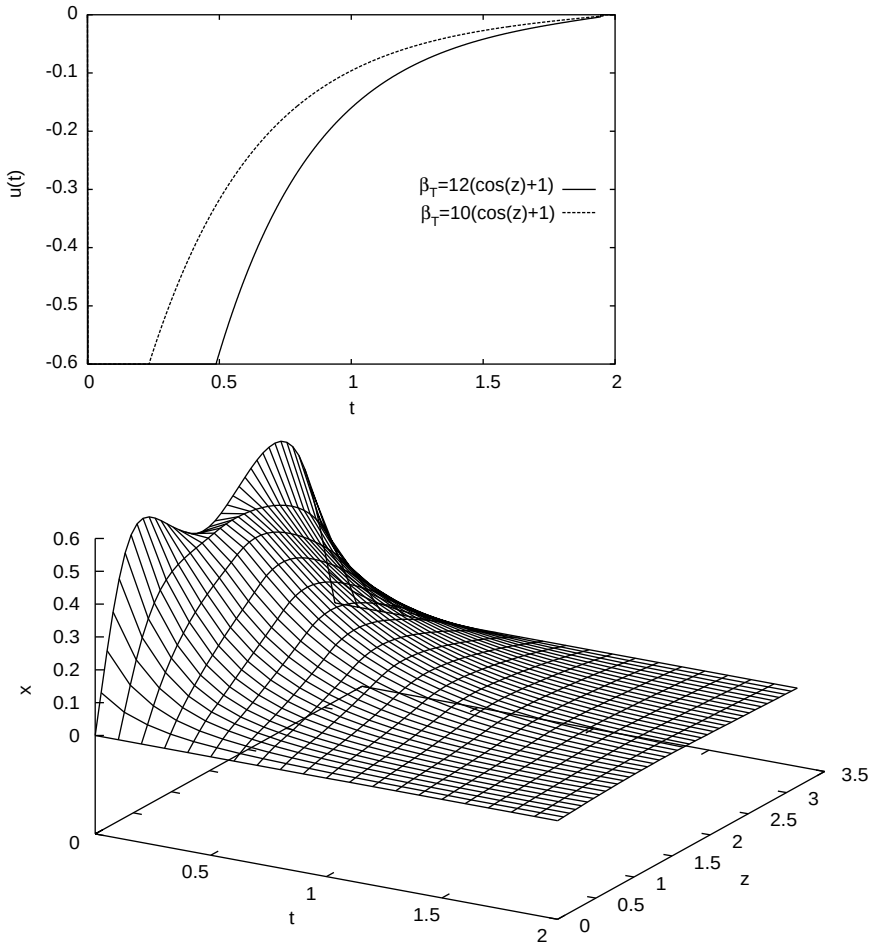

Fig. 20. (Top plot) Profiles of $u(t)$ in the case of using the first set of empirical eigenfunctions as basis functions: -12.5% variation in β_T. (Bottom plot) Profile of the state of the PDE of Eq. (32) for optimal $u(t)$ ($N = 3$).

empirical eigenfunctions can be used to solve more optimization problems than the ones reported here, thereby significantly reducing the fraction of the time needed to compute the empirical eigenfunctions. The time needed to compute the empirical eigenfunctions is the sum of the time needed to construct the ensemble of snapshots and the time needed to compute the empirical eigenfunctions through application of K–L expansion to the ensemble. For the first set of empirical eigenfunctions, this time was on the order of 100 s and for the second set of empirical eigenfunctions on the order of 1000 s.

5. Spatial discretization using approximate inertial manifolds

5.1. Computation of approximate dynamic optimization programs

In this section, we propose an approach to the solution of the program of Eq. (5) which is based on combination of the method of weighted residuals with the concept of approximate inertial manifolds. Following the derivation of a large-scale discretization of the PDE system using the method of weighted residuals (consider the dynamic nonlinear program of Eq. (8) with N large), the central idea is to maintain the dynamics of the dominant modes and neglect the dynamics of the modes corresponding to fast dynamics (i.e., reduce the ODE system that describes the dynamics of the higher-order (fast) eigenmodes to an algebraic one). For certain highly dissipative PDE systems, a rigorous justification of this approximation can be obtained within the framework of inertial manifolds (see (Foias, Sell, & Temam, 1988b) for the detailed mathematical development of this concept) and approximate inertial manifolds (see (Foias, Manley, & Temam, 1988a; Foias, Jolly, Kevrekidis, Sell, & Titi, 1989) for approaches to construction and computation of approximate inertial manifolds, and also (Christofides & Daoutidis, 1997; Christofides, 2001) for the use of approximate inertial manifolds in feedback control of parabolic PDE systems). This approximation leads to a dynamic nonlinear program whose equality constraints

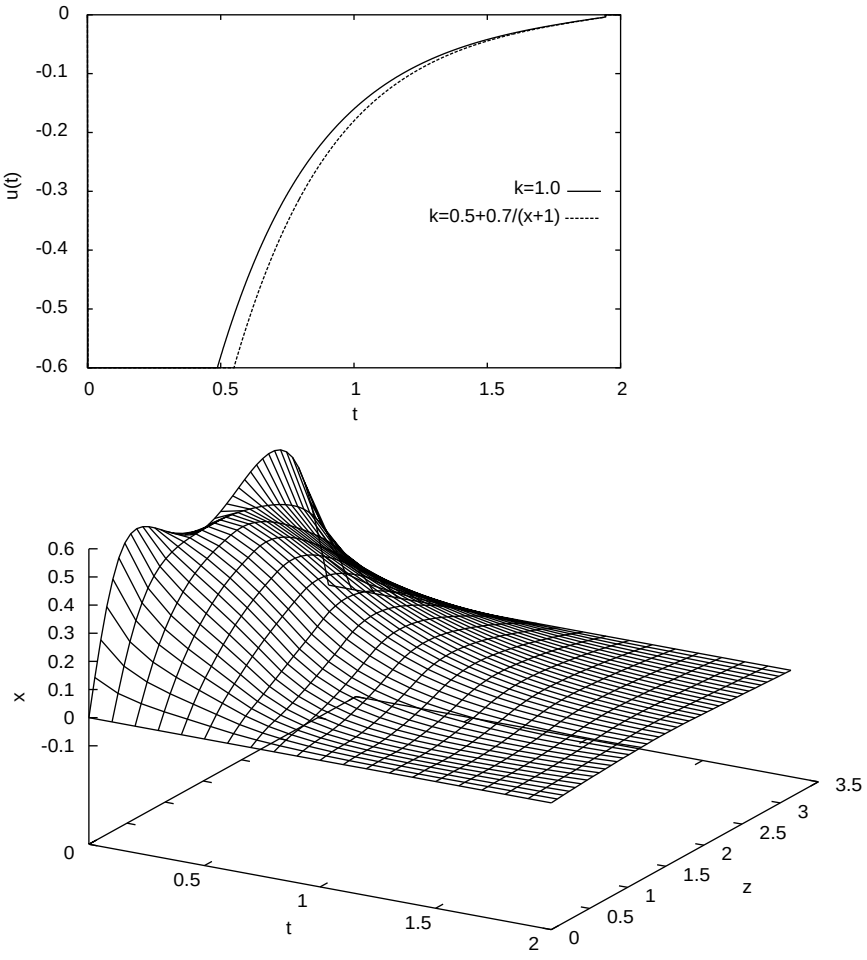

Fig. 21. (Top plot) Profiles of $u(t)$ in the case of using the first set of empirical eigenfunctions as basis functions—$k = 1.0$ (linear spatial differential operator). (Bottom plot) Profile of the state of the PDE of Eq. (32) for optimal $u(t)$ ($N = 3$).

constitute a low-order system of coupled ordinary differential equations and algebraic equations (DAEs) which can then be solved with combination of standard temporal discretization and nonlinear programming techniques. To present this procedure, we consider the optimization program of Eq. (9) and let $a_s(t)$ be the vector of the modes that are associated with the dominant dynamics of the PDE system and $a_f(t)$ be the modes that are associated with dynamics that decay very fast but are important in terms of capturing the long-time behavior of the PDE. Using this decomposition, the dynamic nonlinear program of Eq. (9) can be written as

$$\begin{aligned} \min \quad & \int_0^{t_f} G(a_s, a_f, d)\,\mathrm{d}t \\ \text{s.t.} \quad & \dot{a}_s = \tilde{f}_s(a_s, a_f, d), \\ & \dot{a}_f = \tilde{f}_f(a_s, a_f, d), \\ & \tilde{g}(a_s, a_f, d) \leqslant 0. \end{aligned} \tag{35}$$

Since the dynamics of the fast modes decay very fast, we can formally set the time-derivative of a_f equal to zero (i.e., pretend that the "fast" variables are in fact stationary Haken, 1978) to obtain the following approximate program:

$$\begin{aligned} \min \quad & \int_0^{t_f} G(a_s, a_f, d)\,\mathrm{d}t \\ \text{s.t.} \quad & \dot{a}_s = \tilde{f}_s(a_s, a_f, d), \\ & 0 = \tilde{f}_f(a_s, a_f, d), \\ & \tilde{g}(a_s, a_f, d) \leqslant 0. \end{aligned} \tag{36}$$

The combination of the method of weighted residuals and approximate inertial manifolds for the spatial discretization of dynamic NLPs with parabolic PDE constraints offers a number of advantages over spatial discretization with standard (linear) Galerkin's method. First, the constructed algebraic constraints are integrated to the ODE system leading to a lower number of variables that need to be discretized in the temporal domain. Second, the proposed method enables us to use larger time-discretization steps while maintaining stability of the discretization, since the resulting differential-algebraic-equation system is not as stiff, due to the fact that the dynamics of the slow modes are retained and the dynamics of the fast modes are neglected. Since the

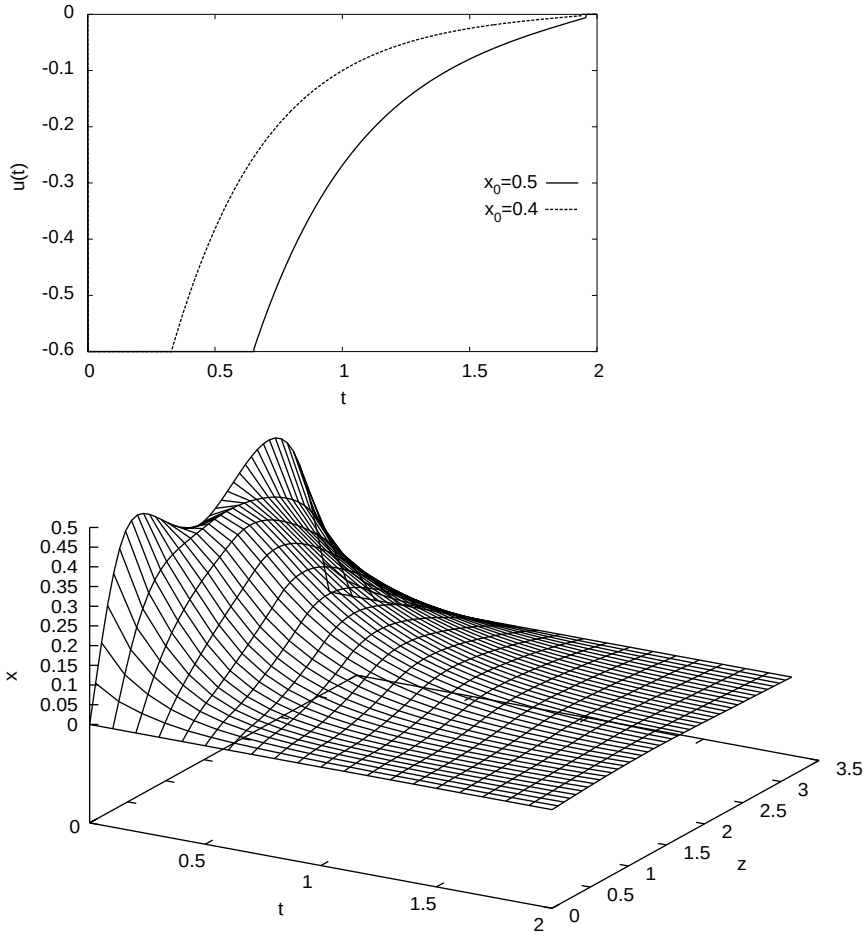

Fig. 22. (Top plot) Profiles of $u(t)$ in the case of using the first set of empirical eigenfunctions as basis functions—20% variation in x_0. (Bottom plot) Profile of the state of the PDE of Eq. (32) for optimal $u(t)$ ($N = 3$).

algebraic equality constraints in the dynamic nonlinear program of Eq. (36) can be numerically solved for a_f, the computation of the optimal solution can be accomplished by following the procedure presented in Sections 3.2 and 3.3 (details are omitted for brevity).

Remark 14. When there is a need to capture the evolution of the fast transients, one can complement the dynamic nonlinear program of Eq. (36) with an approximation of the dynamic nonlinear program of Eq. (35) that captures its behavior in the short-time interval, $[0, \tau_f]$, needed for the dynamics of the fast modes to settle. This approximate nonlinear program can be used to compute $d(t)$ in the interval, $[0, \tau_f]$, and has the following form:

$$\begin{aligned} \min \quad & \int_0^{\tau_f} G(a_s(0), a_f(t), d)\,\mathrm{d}t \\ \text{s.t.} \quad & \dot{a}_f = \tilde{f}_f(a_s(0), a_f(t), d), \\ & \tilde{g}(a_s(0), a_f(t), d) \leqslant 0. \end{aligned} \tag{37}$$

With the above formulation, one can solve the above program to compute $d(t)$ in the interval, $[0, \tau_f]$, and then solve the nonlinear program of Eq. (36) to compute $d(t)$ in the interval, $[\tau_f, t_f]$. This type of two-time-scale decomposition may be useful when the initial conditions associated with the fast modes are far from the equilibrium manifold and, therefore, the approximation $0 = \tilde{f}_f(a_s, a_f, d)$ is not valid for short times. This two-time-scale decomposition also allows eliminating the stiffness problems associated with the temporal integration of the differential equations included in the nonlinear program of Eq. (35) by having to integrate sets of nonstiff differential equations evolving in separate time-scales. The accuracy of this two-time-scale decomposition of the nonlinear program of Eq. (35) can be improved by increasing the separation between the slow and fast modes; for certain PDE systems, this can be always accomplished by increasing the number of modes included in the slow set.

5.2. Application to Kuramoto–Sivashinsky equation

In this section, we present an application of the proposed optimization method to the Kuramoto–Sivashinsky equation

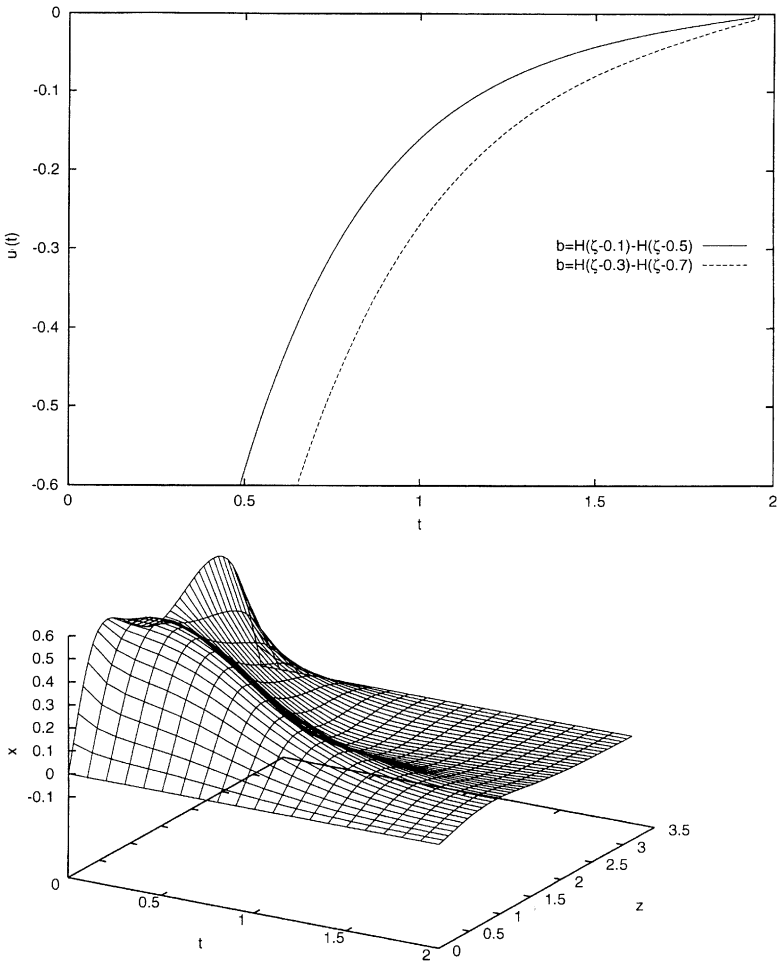

Fig. 23. (Top plot) Profiles of $u(t)$ in the case of using the first set of empirical eigenfunctions as basis functions—$b(\zeta) = H(\zeta - 0.3) - H(\zeta - 0.7)$. (Bottom plot) Profile of the state of the PDE of Eq. (32) for optimal $u(t)$ ($N = 3$).

with distributed actuation

$$\frac{\partial x}{\partial t} = -v\frac{\partial^4 x}{\partial z^4} - \frac{\partial^2 x}{\partial z^2} - x\frac{\partial x}{\partial z} + b(z)u(t) \tag{38}$$

subject to the periodic boundary conditions:

$$\frac{\partial^j x}{\partial z^j}(-\pi, t) = \frac{\partial^j x}{\partial z^j}(+\pi, t), \quad j = 0, \ldots, 3 \tag{39}$$

and the initial condition

$$x(z, 0) = x_0(z), \tag{40}$$

where $x(z,t)$ is the state of the system, $z \in [-\pi, \pi]$ is the spatial coordinate, t is the time and 2π is the length of the spatial domain, v is the instability parameter, $x_0(z)$ is the initial condition, $u(t)$ is the magnitude of the actuation, and $b(z)$ is the actuator distribution function. A direct computation of the solution of the above eigenvalue problem for the spatial differential operator yields $\lambda_0 = 0$ with $\psi_0(z) = 1/\sqrt{2\pi}$, and $\lambda_n = -vn^4 + n^2$ (λ_n is an eigenvalue of multiplicity two) with eigenfunctions $\phi_n(z) = (1/\sqrt{\pi})\sin(nz)$ and $\psi_n(z) = (1/\sqrt{\pi})\cos(nz)$ for $n = 1, \ldots, \infty$. We also define the eigenspectrum of $\mathscr{A}$, $\sigma(\mathscr{A})$, as the set of all eigenvalues of $\mathscr{A}$, i.e. $\sigma(\mathscr{A}) = \{\lambda_1, \lambda_2, \ldots, \}$. From the expression for the eigenvalues, it follows that for a fixed value of $v > 0$ the number of unstable eigenvalues of $\mathscr{A}$ is finite and the distance between two consecutive eigenvalues increases as n increases. This implies that for a fixed value of $v > 0$, the dominant dynamics of the KSE can be described by a finite-dimensional system.

First, we set $v = 0.12$ and consider an initial condition of the form $x_0(z) = \sum_{j=1}^{4} [\sin(j\,z)]$. For $v = 0.12$, the spatially uniform steady state, $x(z,t) = 0$ is unstable (see Fig. 27). Therefore, we formulate the optimization problem as the one of computing an optimal input trajectory $u(t)$ for the actuator such that a meaningful cost that includes penalty on the process response and the control action is minimized, in the presence of constraints in the magnitude of the actuation. Mathematically, this optimization problem is formulated as follows:

$$\min J = \int_0^{t_f} \int_{-\pi}^{\pi} (w_s x^2 + w_u u^2)\, \mathrm{d}z\, \mathrm{d}t,$$

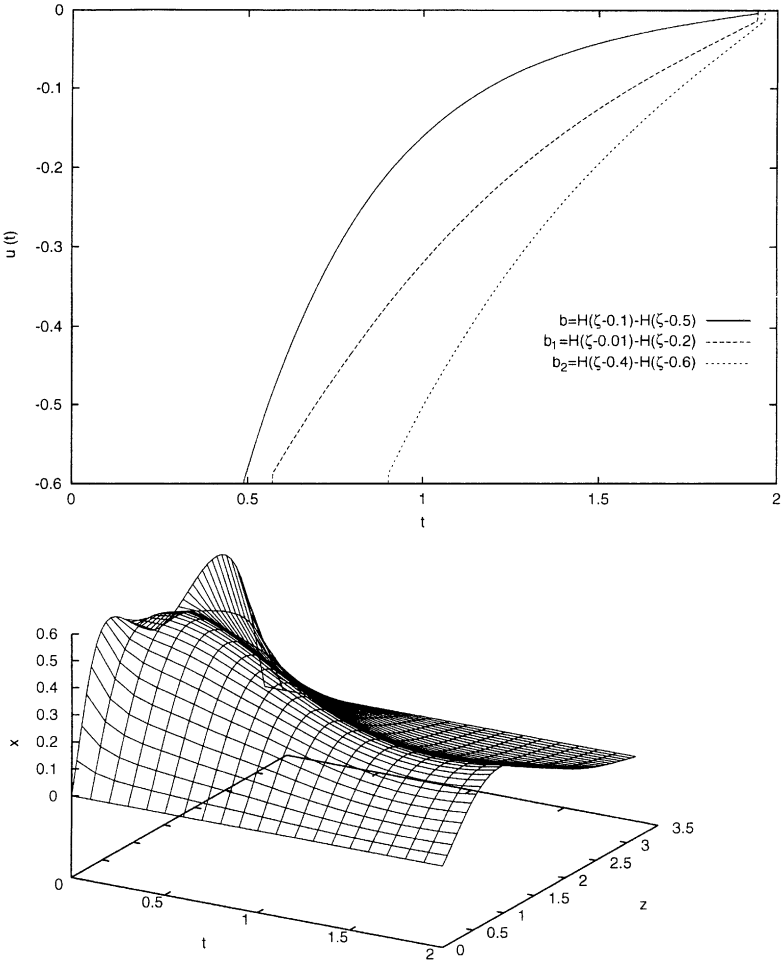

Fig. 24. (Top plot) Profiles of $u(t)$ in the case of using the first set of empirical eigenfunctions as basis functions—two control actuators with $b_1(\zeta)=H(\zeta-0.01)-H(\zeta-0.2)$ and $b_2(\zeta)=H(\zeta-0.4)-H(\zeta-0.6)$. (Bottom plot) Profile of the state of the PDE of Eq. (32) for optimal $u(t)$ ($N=3$).

$$\frac{\partial x}{\partial t} = -v\frac{\partial^4 x}{\partial z^4} - \frac{\partial^2 x}{\partial z^2} - x\frac{\partial x}{\partial z} + b(z)u(t),$$

$$\frac{\partial^j x}{\partial z^j}(-\pi,t) = \frac{\partial^j x}{\partial z^j}(+\pi,t), \quad j=0,\ldots,3,$$

$$x(z,0) = \sum_{j=1}^{4}[\sin(j\,z)], \quad |u(t)| \leqslant M, \tag{41}$$

where $M = 3.0$, $w_s = 100$ and $w_u = 20$. We initially computed an optimal solution to the above problem by performing spatial discretization using Galerkin's method with the eigenfunctions of the spatial differential operator as basis functions and temporal discretization using implicit Euler. For $v = 0.12$ and $x_0(z) = \sum_{j=1}^{4}[\sin(j\,z)]$ (type 1), two actuators with $b_1(z) = \delta(z + 0.5\pi)$ and $b_2(z) = \delta(z - 0.5\pi)$ (point actuation applied at $z = -0.5\pi$ and $z = 0.5\pi$) were used. Optimal solution profiles of $u(t)$ were computed for different numbers of basis functions (in all these cases the step of temporal discretization was appropriately adjusted to guarantee numerical stability of the temporal integration) to obtain a convergent solution profile. Fig. 28 (top plots) shows optimal solution profiles of $u(t)$, for $N = 3, 5, 6$. Clearly, these profiles converge to a single optimal profile, for $N = 6$; note that $u(t)$ satisfies $|u(t)| \leqslant 3.0$. Fig. 28 (bottom plot) shows the profile of the state $x(z,t)$ for $N = 6$; it is clear that the optimal input profile leads to operation of the process close to the spatially uniform steady state at a finite time. As in the case of the diffusion-reaction process, the time needed to solve the optimization problem (Table 3) is the fraction of the time needed to solve this problem when spatial discretization is performed using finite differences. We also used the proposed combination of Galerkin's method with approximate inertial manifolds to solve the optimization problem of Eq. (41) for the same initial condition. First, the standard combination of Galerkin's method with approximate inertial manifolds, formulation of Eq. (36), was used. Fig. 29 (top plots) shows optimal solution profiles of $u(t)$ for different orders of approximation. Clearly, these profiles converge to the single optimal profile of Eq. (28). Fig. 29 (bottom plot)

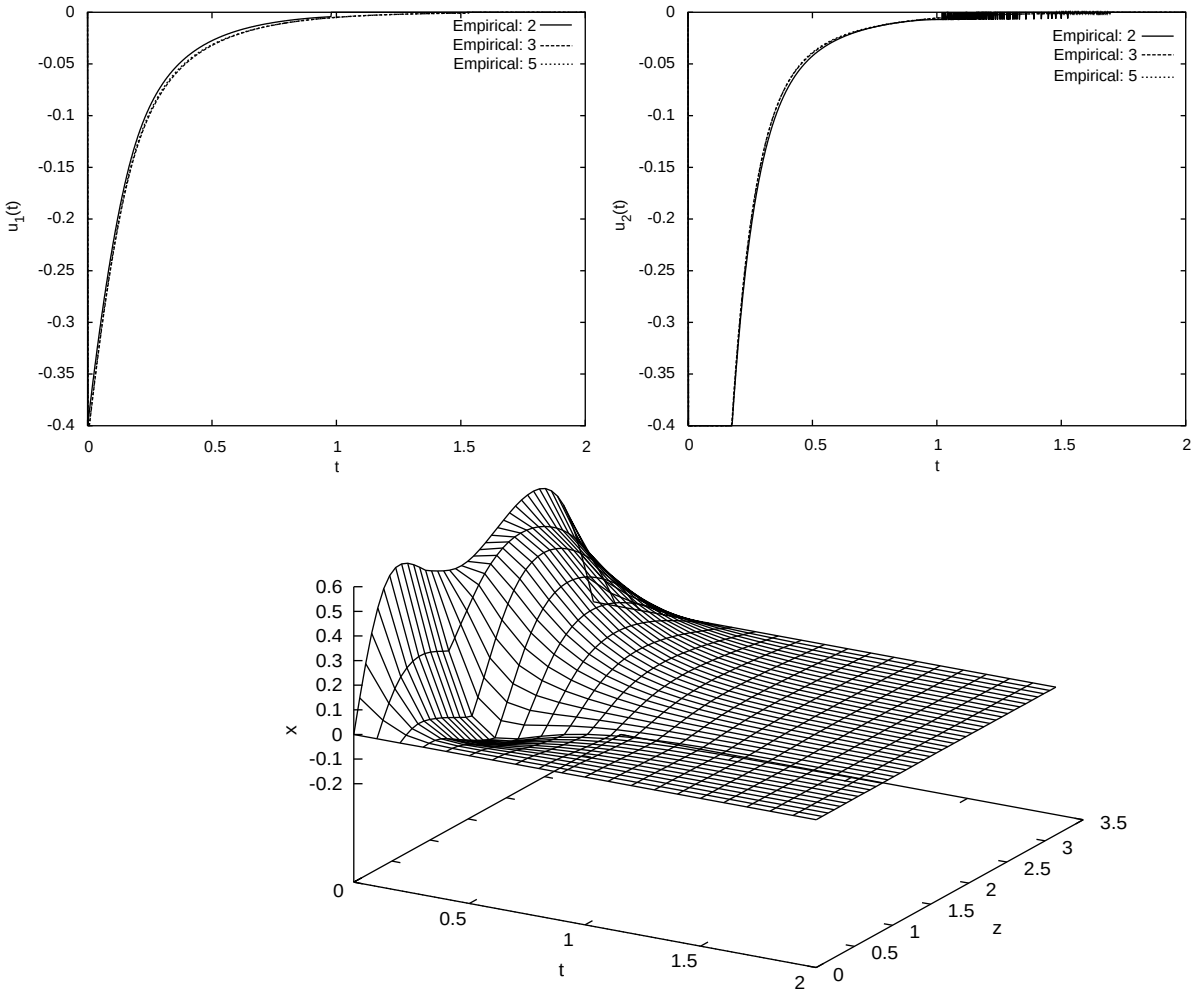

Fig. 25. (Top plots) Profiles of $u(t)$ in the case of using the second set of empirical eigenfunctions as basis functions—two control actuators with $b_1(\zeta) = H(\zeta - 0.1) - H(\zeta - 0.5)$ and $b_2(\zeta) = \delta(\zeta - 0.3)$. (Bottom plot) Profile of the state of the PDE of Eq. (32) for optimal $u(t)$ ($N = 3$).

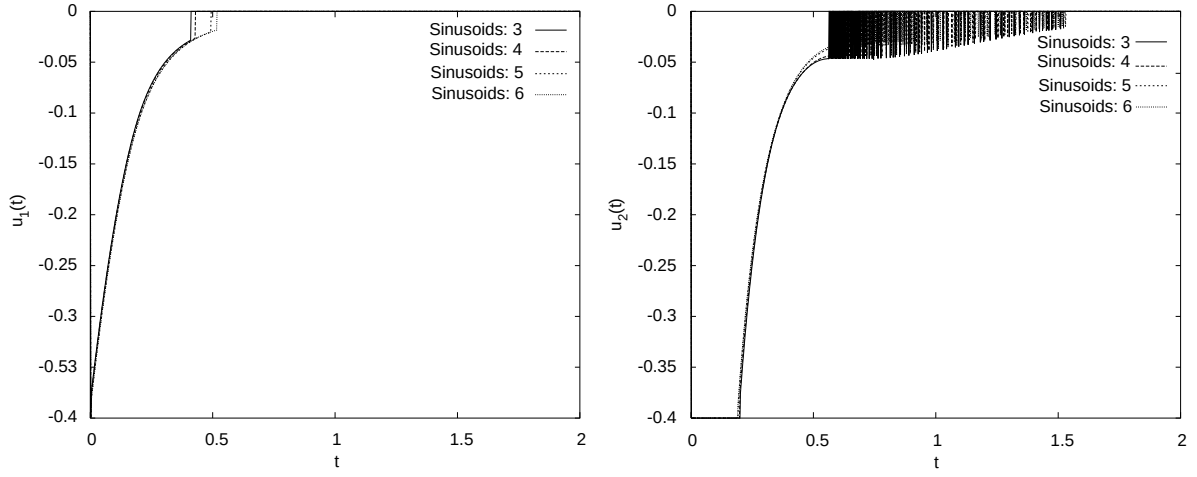

Fig. 26. Profiles of $u(t)$ in the case of using sinusoidal basis functions—two control actuators with $b_1(\zeta) = H(\zeta - 0.1) - H(\zeta - 0.5)$ and $b_2(\zeta) = \delta(\zeta - 0.3)$.

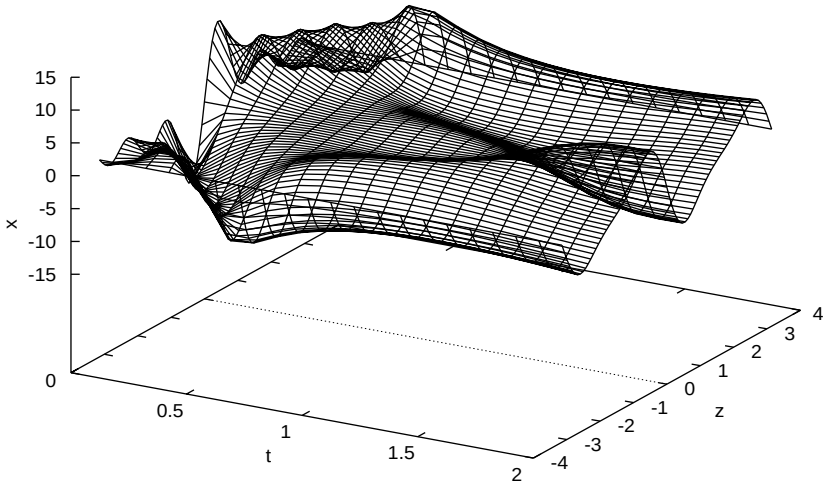

Fig. 27. Profile of the state of the KSE for $\nu = 0.12$.

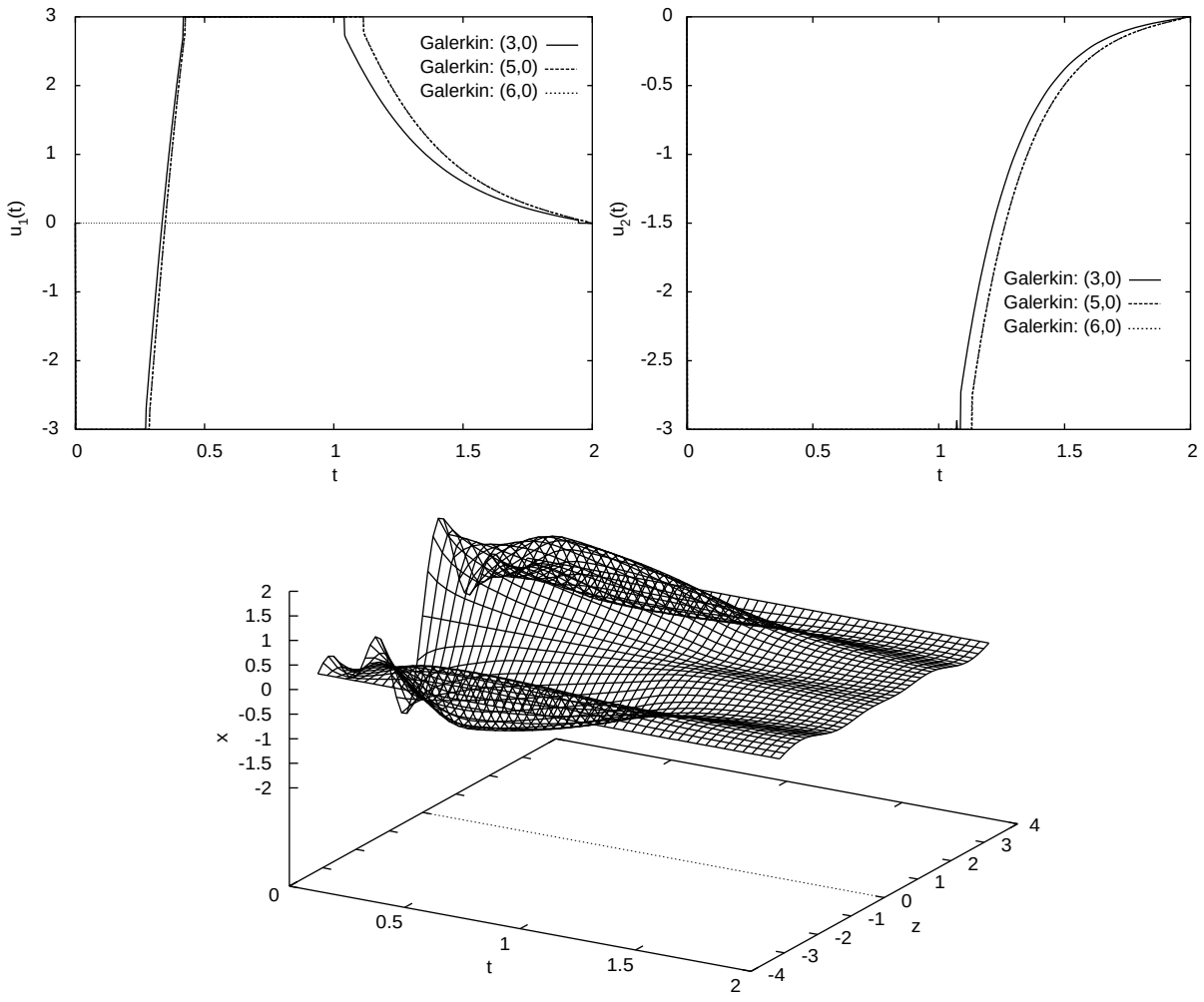

Fig. 28. (Top plots) Profiles of $u(t)$ in the case of using Galerkin's method with sinusoidal basis functions—$x_0 = \sum_{i=1}^{4} \sin(iz)$. (Bottom plot) Profile of the state of the KSE for optimal $u(t)$ ($N = 6$).

Table 3
Optimization results for Kuramoto–Sivashinsky equation with $\nu = 0.12$

Number/type of basis functions	Initial condition	Design variables	Objective	Time (s)	Fig.
3+0/Galerkin	Type 1	2	39.3636	114.4	28
5+0/Galerkin	Type 1	2	43.9868	1530.9	28
6+0/Galerkin	Type 1	2	44.0242	710.9	28
3+5/Galerkin+AIM	Type 1	2	38.6164	1844.5	29
4+4/Galerkin+AIM	Type 1	2	44.0829	1401.9	29
4+6/Galerkin+AIM	Type 1	2	44.0826	3809.4	29
5+3/Galerkin+AIM	Type 1	2	44.0106	1930.5	29
3+5/Galerkin+eAIM	Type 1	2	43.8599	1787.6	30
4+4/Galerkin+eAIM	Type 1	2	44.1915	1492.4	30
4+6/Galerkin+eAIM	Type 1	2	44.0826	3802.8	30
5+3/Galerkin+eAIM	Type 1	2	44.0107	4305.8	30
3+0/Galerkin	Type 2	2	31.5730	282.8	31
4+0/Galerkin	Type 2	2	43.0735	428.3	31
5+0/Galerkin	Type 2	2	47.3991	690.5	31
6+0/Galerkin	Type 2	2	50.6064	1053.5	31
2+6/Galerkin+AIM	Type 2	2	65.2695	1565.1	32
3+5/Galerkin+AIM	Type 2	2	32.2441	2118.0	32
5+5/Galerkin+AIM	Type 2	2	47.6562	4466.4	32
2+6/Galerkin+eAIM	Type 2	2	51.3738	1444.1	33
3+5/Galerkin+eAIM	Type 2	2	49.8594	2313.0	33
5+5/Galerkin+eAIM	Type 2	2	50.2378	5213.3	33

shows the profile of the state $x(z,t)$. Subsequently, the proposed combination of Galerkin's method with modified approximate inertial manifolds, formulation of Eq. (37), was used. Figure 30 (top plots) shows optimal solution profiles of $u(t)$ for different orders of approximation. Clearly, these profiles converge to the single optimal profile of Eq. (28). Fig. 30 (bottom plot) shows the profile of the state $x(z,t)$.

Finally, we used the proposed optimization methods to solve the program of Eq. (41) for a different initial condition, namely $x_0 = 0.5\sum_{i=1}^{3}\sin(iz) + 1.5\sum_{i=4}^{6}\sin(iz)$ (type 2). We initially tried to compute an optimal solution to the above problem by performing spatial discretization using Galerkin's method with the eigenfunctions of the spatial differential operator (sinusoidal functions) as basis functions and temporal discretization using implicit Euler. Optimal solution profiles of $u(t)$ were computed for different numbers of basis functions (in all these cases the step of temporal discretization was appropriately adjusted to guarantee numerical stability of the temporal integration). Fig. 31 shows solution profiles of $u(t)$, for $N = 3,4,5,6$. Clearly, these profiles show that convergence to a single optimal profile improves as more basis functions are used. However, even for $N = 6$, convergence of the input $u_1(t)$ to the optimal profile has not been obtained, and it is clear that a higher-order discretization is needed to obtain a convergent profile for $u_1(t)$. To be able to achieve convergence with a low-order approximation, we subsequently used the proposed combination of Galerkin's method with approximate inertial manifolds to solve the optimization problem for the same initial condition. Fig. 32 (top plots) shows solution profiles of $u(t)$ for different orders of approximation. Clearly, these profiles converge to a single optimal profile; note the small difference (especially for small times) in the optimal solution profiles for $u_1(t)$ and $u_2(t)$ between the $(3,5)$ and $(5,5)$ dynamic nonlinear programs. Fig. 32 (bottom plot) shows the profile of the state $x(z,t)$ under the $u(t)$ obtained from the solution of the $(5,5)$ dynamic nonlinear program. It is clear that the optimal input profile leads to operation of the process close to the spatially uniform steady state at a finite time. The time needed to solve the optimization problem using this approach is the fraction of the time needed to solve this problem when spatial discretization is performed using finite differences or through a high-order truncation obtained via linear Galerkin's method (Table 3). Finally, to further improve the accuracy of the $(3,5)$ optimization program for small times, the proposed combination of Galerkin's method with modified approximate inertial manifolds, formulation of Eqs. (36)–(37), was used. Fig. 33 (top plots) shows optimal solution profiles of $u(t)$ for different orders of approximation. Clearly, the convergence properties have been substantially improved for small times and the $(3,5)$ and $(5,5)$ optimization programs give identical results. Fig. 33 (bottom plot) shows the profile of the state $x(z,t)$. The optimal input profile again leads to operation of the process close to the spatially uniform steady state at a finite time. We observe that the combination of Galerkin's method and approximate inertial manifolds, as well as the two-time-scale modification of Eq. (37) lead to improved results (in terms of the order of the convergent approximation and the time needed to obtain the optimal solution), compared to discretization using linear Galerkin's method. The reason is that the chosen initial condition excites higher-order modes of

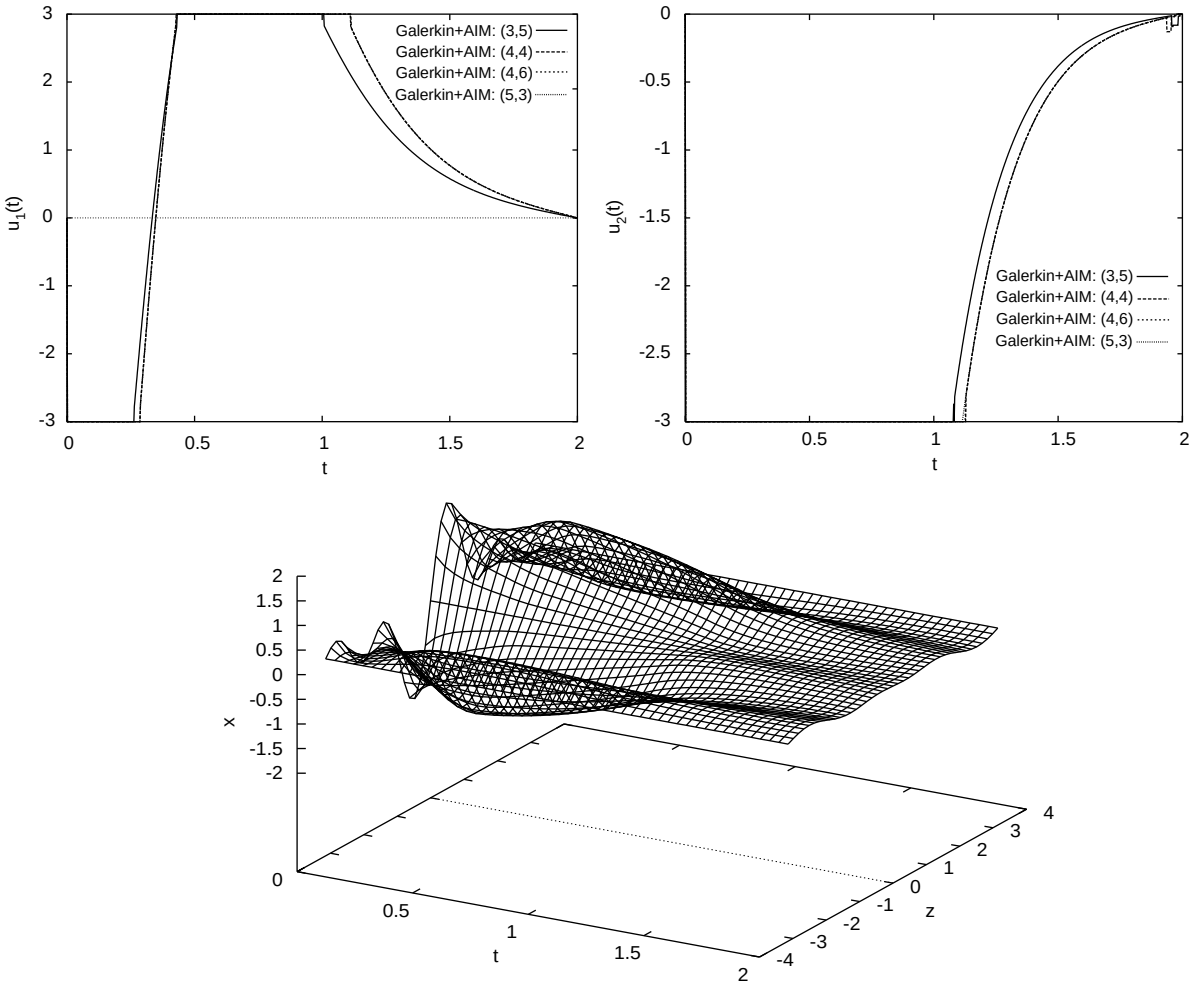

Fig. 29. (Top plots) Profiles of $u(t)$ in the case of spatial discretization using Galerkin's method with approximate inertial manifolds—$x_0 = \sum_{i=1}^{4} \sin(iz)$. (Bottom plot) Profile of the state of the KSE for optimal $u(t)$.

the KSE that cannot be captured with a low-order ODE approximation that does not account at all for the evolution of these higher-order modes.

6. Concluding remarks

This article presented computationally-efficient methods for the solution of *dynamic* constraint optimization problems arising in the context of spatially distributed processes governed by highly dissipative nonlinear partial differential equations (PDEs). The methods are based on spatial discretization using the method of weighted residuals with analytical or empirical (obtained via Karhunen–Loève expansion) eigenfunctions as basis functions, and combination of the method of weighted residuals with approximate inertial manifolds. The proposed methods account for the fact that the dominant dynamics of highly dissipative PDE systems are low dimensional in nature and lead to approximate optimization problems that are of significantly lower order compared to the ones obtained from spatial discretization using finite-difference and finite-element techniques, and thus, they can be solved with significantly smaller computational demand. We used two representative examples of dissipative PDEs, a diffusion-reaction process with constant and spatially varying coefficients, and the Kuramoto–Sivashinsky equation, a model that describes incipient instabilities in a variety of physical and chemical systems, to demonstrate the implementation and evaluate the effectiveness of the proposed optimization algorithms. The robustness of the optimization methods with respect to significant variations in model parameters, initial conditions and actuator distribution functions were successfully tested through extensive numerical simulations.

Finally, we note that although the proposed optimization algorithms worked well for the several test cases considered in this work, significant work remains to be done in applying these algorithms to more complex PDE models of transport-reaction processes and fluid dynamic systems to further evaluate their effectiveness and performance and to eventually establish them as useful tools for dynamic optimization of dissipative PDE systems.

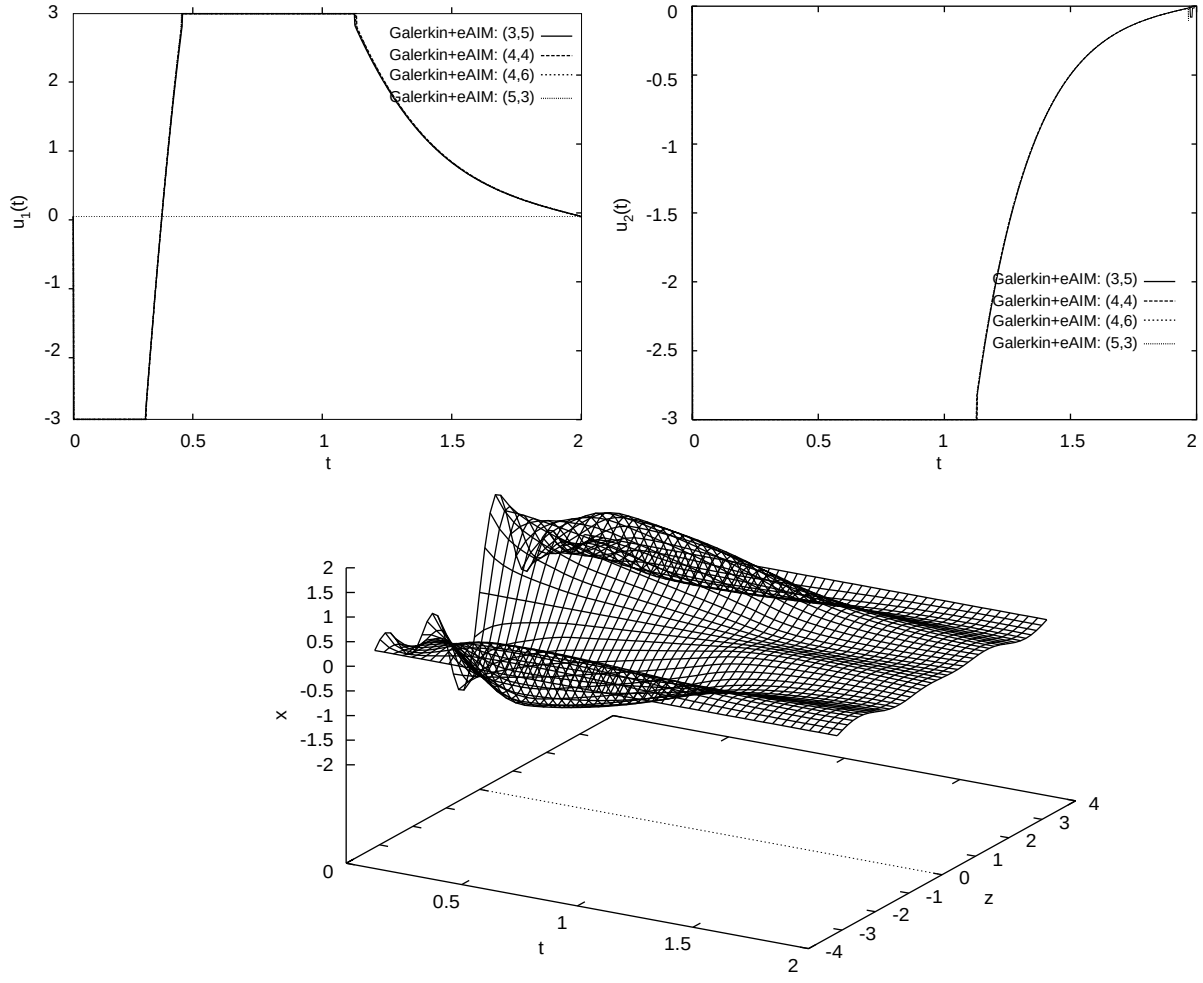

Fig. 30. (Top plots) Profiles of $u(t)$ in the case of spatial discretization using Galerkin's method with modified approximate inertial manifolds—$x_0 = \sum_{i=1}^{4} \sin(iz)$. (Bottom plot) Profile of the state of the KSE for optimal $u(t)$.

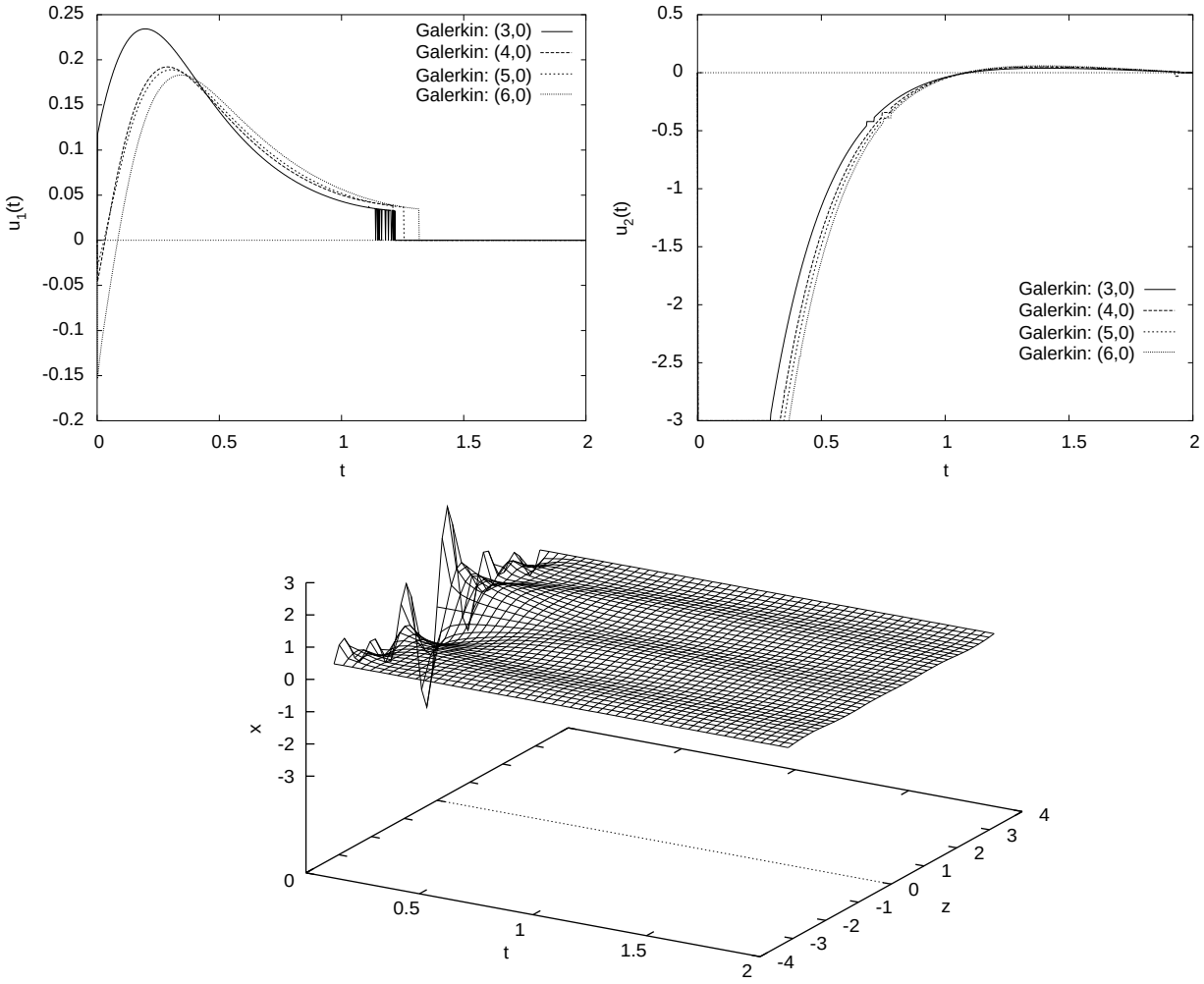

Fig. 31. (Top plots) Profiles of $u(t)$ in the case of spatial discretization using Galerkin's method with modified approximate inertial manifolds—$x_0 = 0.5 \sum_{i=1}^{3} \sin(iz) + 1.5 \sum_{i=4}^{6} \sin(iz)$. (Bottom plot) Profile of the state of the KSE for optimal $u(t)$.

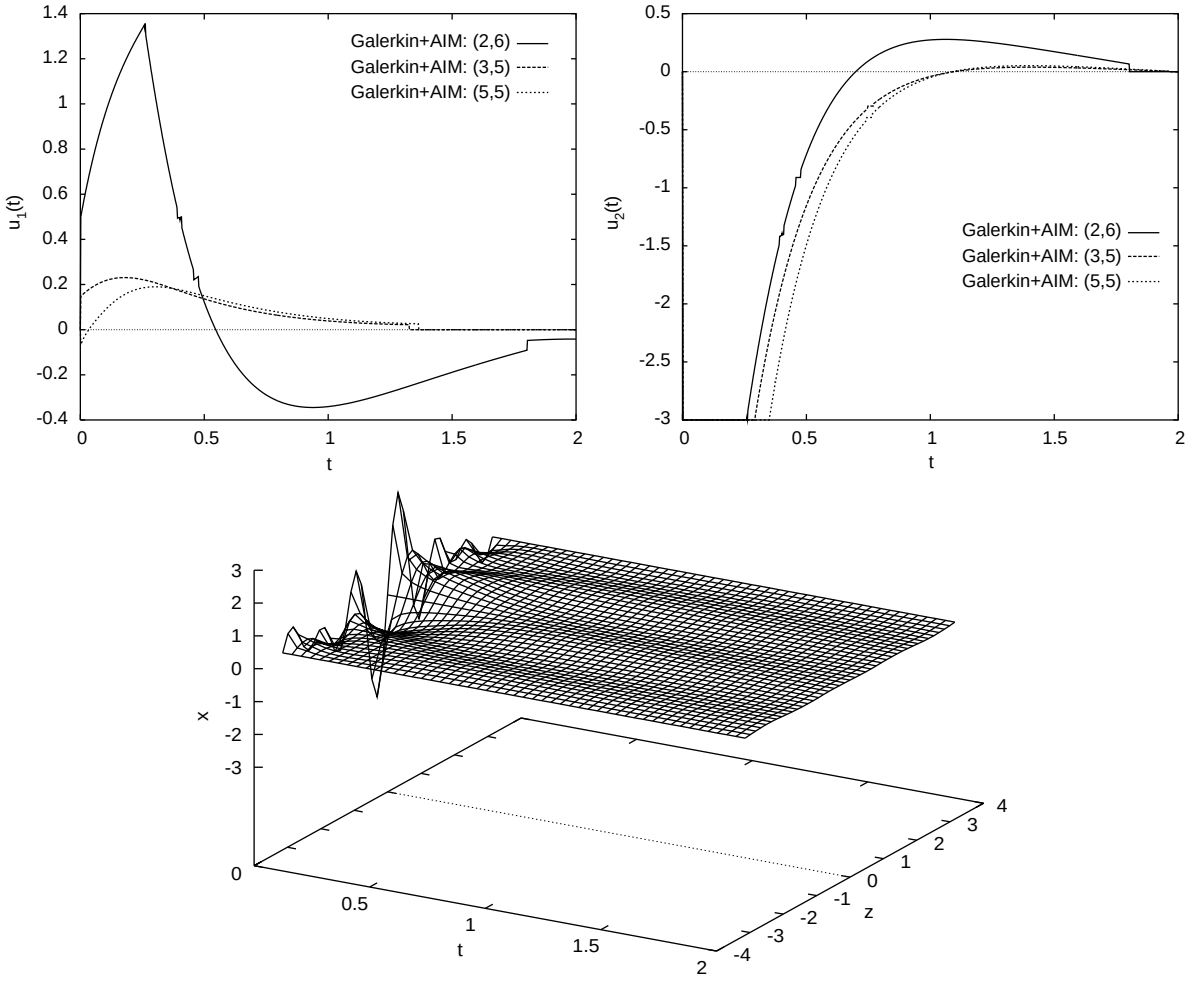

Fig. 32. (Top plots) Profiles of $u(t)$ in the case of spatial discretization using Galerkin's method with approximate inertial manifolds—$x_0 = 0.5 \sum_{i=1}^{3} \sin(iz) + 1.5 \sum_{i=4}^{6} \sin(iz)$. (Bottom plot) Profile of the state of the KSE for optimal $u(t)$.

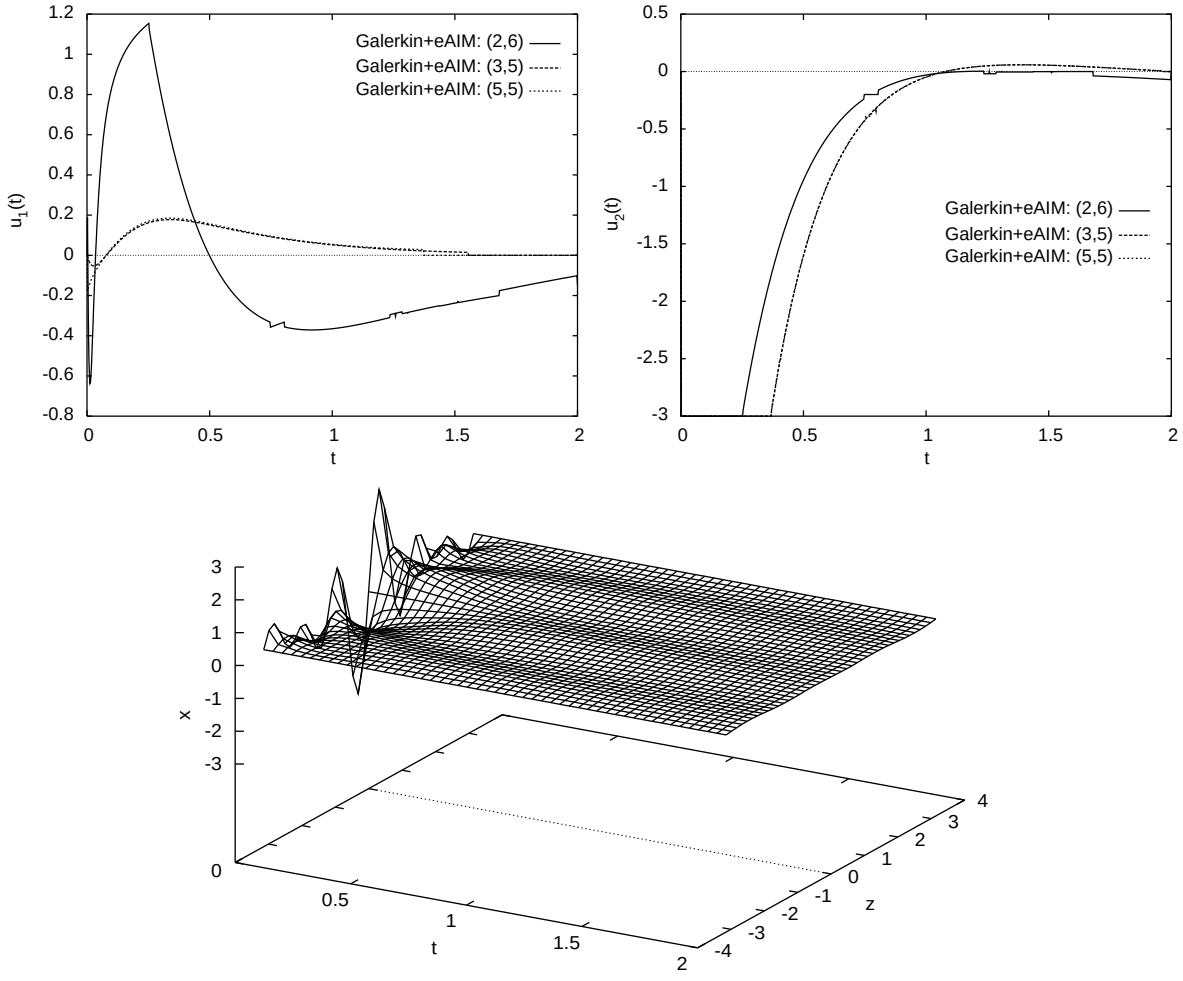

Fig. 33. (Top plots) Profiles of $u(t)$ in the case of using Galerkin's method with sinusoidal basis functions—$x_0 = 0.5 \sum_{i=1}^{3} \sin(iz) + 1.5 \sum_{i=4}^{6} \sin(iz)$. (Bottom plot) Profile of the state of the KSE for optimal $u(t)$ ($N = 6$).

Acknowledgements

Financial support from the National Science Foundation, CTS-0002626, is gratefully acknowledged.

References

Al-Said, E. A., & Noor, M. A. (1998). Numerical solutions of a system of fourth order boundary value problems. *International Journal of Computer Mathematics*, *70*, 347–355.

Al-Said, E. A., Noor, M. A., & Rassias, T. M. (1998). Numerical solutions of third-order obstacle problems. *International Journal of Computer Mathematics*, *69*, 75–84.

Alexandrov, N. M., Dennis, J. E., Lewis, R. M., & Torczon, V. (1998). A trust-region framework for managing the use of approximation models in optimization. *Structural Optimization*, *15*, 16–23.

Arian, E., Fahl, M., & Sachs, E. W. (2000). *Trust-region proper orthogonal decomposition for flow control*. ICASE report no. 2000-25, NASA Langley Research Center, Hampton, VA, USA.

Baker, J., & Christofides, P. D. (2000). Finite dimensional approximation and control of nonlinear parabolic PDE systems. *International Journal of Control*, *73*, 439–456.

Bendersky, E., & Christofides, P. D. (1999). A computationally efficient method for optimization of transport-reaction processes. *Computers & Chemical Engineering*, *23*(s), 447–450.

Bendersky, E., & Christofides, P. D. (2000). Optimization of transport-reaction processes using nonlinear model reduction. *Chemical Engineering Science*, *55*, 4349–4366.

Bertsekas, D. P. (1995). *Nonlinear programming*. Belmont, MA: Athena Scientific.

Biegler, L. T., Grossman, I. E., & Westerberg, A. W. (1997). *Systematic methods of chemical process design*. Englewood Cliffs, NJ: Prentice-Hall.

Biegler, L. T., Nocedal, J., & Schmid, C. (1995). Reduced hessian strategies for large-scale nonlinear programming. *SIAM Journal on Optimization*, *5*, 314.

Borggaard, J., & Burns, J. (1997). A PDE sensitivity equation method for optimal aerodynamic design. *Journal of Computational Physics*, *136*, 366–384.

Chou, S. H., & Porsching, T. A. (1998). A note on the restarted cg method and reduced space additive correction. *Computers & Mathematics with Applications*, *35*, 129–136.

Christofides, P. D. (2001). *Nonlinear and robust control of PDE systems: Methods and applications to transport-reaction processes*. Boston: Birkhäuser.

Christofides, P. D., & Daoutidis, P. (1997). Finite-dimensional control of parabolic PDE systems using approximate inertial manifolds. *Journal of Mathematical Analysis and Applications*, *216*, 398–420.

Dennis, J. E., El-Alem, M., & Maciel, M. C. (1997). A global convergence theory for general trust-region-based algorithms for equality constrained optimization. *SIAM Journal on Optimization*, *7*, 177–207.

Dennis, J. E., El-Alem, M., & Williamson, K. (1999). A trust-region approach to nonlinear systems of equalities and inequalities. *SIAM Journal on Optimization*, *9*, 291–315.

Finlayson, B. A. (1980). *Nonlinear analysis in chemical engineering*. New York: McGraw-Hill.

Floudas, C. A., & Panos, M. P. (1992). *Recent advances in global optimization*. Princeton, NJ: Princeton University Press.

Foias, C., Jolly, M. S., Kevrekidis, I. G., Sell, G. R., & Titi, E. S. (1989). On the computation of inertial manifolds. *Physics Letters A*, *131*, 433–437.

Foias, C., Manley, O., & Temam, R. (1988a). Modelling of the interaction of small and large eddies in two dimensional flows. *Mathematical Modeling 2nd Numerical Analysis*, *22*, 93–114.

Foias, C., Sell, G. R., & Temam, R. (1988b). Inertial manifolds for nonlinear evolution equations. *Journal of Differential Equation*, *73*, 309–353.

Fukunaga, K. (1990). *Introduction to statistical pattern recognition*. New York: Academic Press.

Graham, M. D., & Kevrekidis, I. G. (1996). Alternative approaches to the Karhunen–Loéve decomposition for model reduction and data analysis. *Computers & Chemical Engineering*, *20*, 495–506.

Haken, H. (1978). *Synergetics*. Berlin: Springer.

Hall, C. A., Porsching, T. A., & Mesina, G. L. (1992). On a network method for unsteady incompressible fluid-flow on triangular grids. *International Journal of Numerical Methods in Fluids*, *15*, 1383–1406.

Holmes, P., Lumley, J. L., & Berkooz, G. (1996). *Turbulence, coherent structures, dynamical systems and symmetry*. New York: Cambridge University Press.

Kelley, C. T., & Sachs, E. W. (1999). A trust region method for parabolic boundary control problems. *SIAM Journal of Optimization*, *9*, 1064–1081.

King, B. B., & Sachs, E. W. (2000). Semidefinite programming techniques for reduced order systems with guaranteed stability margins. *Computational Optimization and Applications*, *17*, 37–59.

Lumley, J. L. (1981). Coherent structures in turbulence. In *Transition and turbulence* (pp. 215–242). New York: Academic Press.

Mahadevan, N., & Hoo, K. A. (2000). Wavelet-based model reduction of distributed parameter systems. *Chemical Engineering Science*, *55*, 4271–4290.

Manousiouthakis, V., & Sourlas, D. (1992). Global optimization approach to rationally constrained rational programming problems. *Chemical Engineering Communications*, *115*, 127–147.

Marquardt, W. (2002). Nonlinear model reduction for optimization based control of transient chemical processes. In J. B. Rawlings, B. A. Ogunnaike, & J. W. Eaton (Eds.), *AIChE Symposium Series*, *Proceedings of chemical process control—6*, Vol. 98 (pp. 12–42).

Miletta, P. D. (1994). Approximation to solutions of evolution equations. *Mathematical Methods in the Applied Science*, *17*, 753–763.

Park, H. M., & Lee, J. H. (1998). A method of solving inverse convection problems by means of model reduction. *Chemical Engineering Science*, *53*, 1731–1744.

Rabier, P. J., & Rheinboldt, W. C. (1995). On the numerical solution of the Euler–Lagrange equations. *SIAM Journal on Numerical Analysis*, *32*, 318–329.

Ray, W. H. (1981). *Advanced process control*. New York: McGraw-Hill.

Rheinboldt, W. C. (1993). On the theory and error estimation of the reduced basis method for multiparameter problems. *Nonlinear Analysis—Theory Methods & Applications*, *21*, 849–858.

Shvartsman, S. Y., & Kevrekidis, I. G. (1998). Nonlinear model reduction for control of distributed parameter systems: A computer assisted study. *A.I.Ch.E. Journal*, *44*, 1579–1595.

Sirovich, L. (1987a). Turbulence and the dynamics of coherent structures. Part I: Coherent structures. *Quarterly Applied Mathematics*, *XLV*, 561–571.

Sirovich, L. (1987b). Turbulence and the dynamics of coherent structures. Part II: Symmetries and transformations. *Quarterly Applied of Mathematics*, *XLV*, 573–582.

Temam, R. (1988). *Infinite-dimensional dynamical systems in mechanics and physics*. New York: Springer.

Turgeon, E., Pelletier, D., & Borggaard, J. (2000). A continuous sensitivity equation approach to optimal design in mixed convection. *Numerical Heat Transfer Part A—Applications*, *38*, 869–885.

Ulbrich, M., Ulbrich, S., & Heinkenschloss, M. (1999). Global convergence of trust-region interior-point algorithms for infinite-dimensional nonconvex minimization subject to pointwise bounds. *SIAM Journal of Control and Optimization*, *37*, 731–764.

Vasantharajan, S., Viswanathan, J., & Biegler, L. T. (1990). Reduced successive quadratic programming implementation for large-scale optimization problems with smaller degrees of freedom. *Computers & Chemical Engineering*, *14*, 907–915.